NACA RM A55C30

NACA

RESEARCH MEMORANDUM

THE EFFECT OF WING HEIGHT ON THE LONGITUDINAL CHARACTERISTICS AT HIGH SUBSONIC SPEEDS OF A WING-FUSELAGE-TAIL COMBINATION HAVING A WING WITH 40° OF SWEEPBACK AND NACA FOUR-DIGIT THICKNESS DISTRIBUTION

By Jerald K. Dickson and Fred B. Sutton

Ames Aeronautical Laboratory
Moffett Field, Calif.

NATIONAL ADVISORY COMMITTEE
FOR AERONAUTICS
WASHINGTON

May 25, 1955
Declassified July 22, 1959

NATIONAL ADVISORY COMMITTEE FOR AERONAUTICS

RESEARCH MEMORANDUM

THE EFFECT OF WING HEIGHT ON THE LONGITUDINAL CHARACTERISTICS AT HIGH SUBSONIC SPEEDS OF A WING-FUSELAGE-TAIL COMBINATION HAVING A WING WITH 40° OF SWEEPBACK AND NACA FOUR-DIGIT THICKNESS DISTRIBUTION

By Jerald K. Dickson and Fred B. Sutton

SUMMARY

A wind-tunnel investigation has been conducted to determine the effect of lowering the wing from the top of the fuselage to the bottom of the fuselage on the longitudinal characteristics of a wing-fuselage and a wing-fuselage-tail combination with the horizontal tail at various heights above the plane of the wing. The wing had 40° of sweepback, an aspect ratio of 7, NACA four-digit thickness distribution, and boundary-layer fences. The tests were conducted through an angle-of-attack range at a Mach number of 0.25 and a Reynolds number of 8 million and at Mach numbers from 0.25 through 0.92 at a Reynolds number of 2 million.

The effects of wing height on the longitudinal characteristics of the model were small. The low-wing configuration generally had slightly more drag, lower drag-divergence Mach numbers, and slightly lower lift-curve slopes than the high-wing configuration. Raising the horizontal tail of the low-wing configuration from the fuselage center line increased the longitudinal stability and the lift coefficient for balance. This increase of tail height also increased the tail-control effectiveness by about 60 percent at a Mach number of 0.80. When mounted on the fuselage center line of the low-wing configuration, the horizontal tail was less effective as a longitudinal control by 37 percent at 0.25 Mach number and by 9 percent at 0.90 Mach number than when mounted on the fuselage center line of the high-wing configuration. However, with the tail above the fuselage center line the control effectiveness was nearly the same for both wing positions.

INTRODUCTION

The longitudinal characteristics of wings suitable for long-range airplanes capable of high subsonic speeds have been the subject of a series of investigations in the Ames 12-foot pressure wind tunnel. Two

twisted and cambered wings of relatively high aspect ratio having either NACA four-digit or NACA 64A thickness distribution with 40°, 45°, and 50° of sweepback have been investigated and the results are presented in reference 1. The wing with four-digit sections was also tested in a high-wing position on a fuselage to determine the effects of various wing fences on the longitudinal-stability characteristics of the wing-fuselage and wing-fuselage-tail combinations. These results are presented in reference 2.

The present phase of the investigations was undertaken to provide a comparison of the longitudinal characteristics of low- and high-wing configurations since many design considerations favor mounting the wing near the bottom of the fuselage. The wing and fuselage of reference 2 were revised to permit the wing with 40° sweepback to be mounted in a low position on the fuselage. This combination was tested with the most satisfactory boundary-layer fences of reference 2 and with an all-movable horizontal tail at several heights and angles of incidence.

NOTATION

A aspect ratio, $\frac{b^2}{2S}$

a mean-line designation, fraction of chord over which design load is uniform

a_t lift-curve slope of the isolated horizontal tail, per deg

a_{w+f} lift-curve slope of the wing-fuselage combination, per deg

a_{w+f+t} lift-curve slope of the wing-fuselage-tail combination, per deg

$\frac{b}{2}$ wing semispan perpendicular to the plane of symmetry

C_D drag coefficient, $\frac{\text{drag}}{qS}$

C_L lift coefficient, $\frac{\text{lift}}{qS}$

C_{L_i} inflection lift coefficient, lowest positive lift coefficient at which $\frac{dC_m}{dC_L} = 0.10$

C_m pitching-moment coefficient about the quarter point of the wing mean aerodynamic chord, $\frac{\text{pitching moment}}{qS\bar{c}}$

c	local chord parallel to the plane of symmetry
c'	local chord perpendicular to the wing sweep axis
$\bar{c}$	mean aerodynamic chord, $\dfrac{\int_0^{b/2} c^2 dy}{\int_0^{b/2} c\, dy}$
c_{l_i}	section design lift coefficient
i_t	incidence of the horizontal tail with respect to the wing root chord
$\frac{L}{D}$	lift-drag ratio
l_t	tail length, longitudinal distance between the quarter points of the mean aerodynamic chords of the wing and the horizontal tail
M	free-stream Mach number
q	free-stream dynamic pressure
R	Reynolds number based on the wing mean aerodynamic chord
S	area of semispan wing
S_t	area of semispan horizontal tail
t	maximum thickness of section
$\bar{V}_t$	horizontal-tail volume, $\dfrac{S_t l_t}{S\bar{c}}$
y	lateral distance from the plane of symmetry
α	angle of attack, measured with respect to a reference plane through the wing root chord and the leading edge
α_t	angle of attack of the isolated horizontal tail
ϵ	effective average downwash angle
λ	taper ratio, ratio of tip chord to root chord
φ	angle of twist, the angle between the local wing chord and the reference plane through the wing leading edge and root chord (positive for washin and measured in planes parallel to the plane of symmetry)

η fraction of semispan, $\frac{y}{b/2}$

$\eta_t\left(\frac{q_t}{q}\right)$ tail efficiency factor (ratio of lift-curve slope of the horizontal tail when mounted on the fuselage in the flow field of the wing to the lift-curve slope of the isolated horizontal tail)

Subscripts

f fuselage

t tail

w wing

Model

The wing-fuselage and wing-fuselage-tail combinations investigated (fig. 1(a)) employed the 40° sweptback, twisted, and cambered wing of reference 2. This wing was constructed of solid steel and had an aspect ratio of 7. The NACA four-digit thickness distribution was combined with an $a = 0.8$ mean line having an ideal lift coefficient of 0.4 to form the sections perpendicular to the reference sweep line (fig. 1(a)). The thickness-chord ratios of these sections varied from 14 percent at the root to 11 percent at the tip as shown in figure 1(b). Twist of 5° (see fig. 1(b)) was built into the wing by rotating the streamwise sections about the leading edge while maintaining the projected plan form.

The fuselage used in the investigation was constructed of aluminum and had a fineness ratio of 12.6 and semicircular cross section. Coordinates of the fuselage are given in table I. The wing was located so that the lower surface at the root was tangent to the bottom of the fuselage. The angle of incidence of the root chord with respect to the body axis was 3°.

The boundary-layer fences used on the upper surface of the wing extended from 0.10 chord to the trailing edge. Details of the fences and their spanwise locations are shown in figure 1(c).

The all-movable horizontal tail had NACA 0010 sections perpendicular to the quarter-chord line, an aspect ratio of 3, a taper ratio of 0.5, and and a sweepback of 40° at the reference sweep line. The axis about which the incidence of the horizontal tail was varied (53.4 percent of the tail root chord) was perpendicular to the plane of symmetry either at or above the fuselage center line. Vertical locations of the horizontal tail, which were the same with respect to the fuselage center line as those of

reference 2, correspond to heights of 13, 20, 26, and 33 percent of the wing semispan above the plane of the wing root chord and leading edge. The tail volume was 0.497 for all positions of the horizontal tail.

A photograph of the low-wing model mounted in the wind tunnel is shown in figure 2 together with a photograph of the high-wing model of reference 2. The turntable upon which the model was mounted connects directly to the balance system.

CORRECTIONS TO DATA

The data have been corrected by the method of reference 3 for constriction effects due to the presence of the tunnel walls, by the method of reference 4 for tunnel-wall interference originating from lift on the model, and for drag tares caused by aerodynamic forces on the turntable upon which the model was mounted.

The corrections to dynamic pressure, Mach number, angle of attack, drag coefficient, and to pitching-moment coefficient were the same as those of reference 2 and are given in table II.

TESTS

The wing-fuselage and the wing-fuselage-tail combinations were tested with the wing and the best fences of reference 2. Tests were conducted at a Mach number of 0.25 and a Reynolds number of 8 million and at Mach numbers from 0.25 to 0.92 and a Reynolds number of 2 million. The height and the angle of incidence of the all-movable horizontal tail were varied.

RESULTS AND DISCUSSION

The large improvements in the longitudinal stability of the high-wing (ref. 2), wing-fuselage combination obtained by use of fences on the wing, indicated that any extensive investigation of the low-wing combination should be conducted with fences on. All the data presented in this report were obtained with the best fences of reference 2 installed on the wing.

Wing-Fuselage Combinations

Low-speed results.- The effects of wing height on the longitudinal characteristics of the wing-fuselage combinations are shown for a Mach

number of 0.25 and a Reynolds number of 8 million in figure 3. The low wing gave a slightly lower lift-curve slope and slightly greater stability than the high wing. The lower value of lift-curve slope for the low wing probably stems from changes in span loading similar to those shown in reference 5 for an unswept wing. A similar change in span loading, on a swept wing, would move the center of pressure outward and rearward and produce the slight increase in longitudinal stability shown.

Less drag was indicated at lift coefficients below about 0.4 for the high position of the wing than for the low position; however, at higher lift coefficients the low-wing configuration usually had slightly less drag. These effects are shown to good advantage by the lift-drag ratios presented in figure 4. Figure 4 also compares lift-drag ratios for Reynolds numbers of 2 million and 8 million. As was expected from the fence-on data of reference 2, the effect of increasing Reynolds number was small, although the low-wing configuration benefited slightly more than did the high-wing configuration from the increase in Reynolds number.

High-speed results.- The longitudinal characteristics of the low-wing and high-wing configurations are compared in figure 5 for Mach numbers from 0.25 to 0.92 and a Reynolds number of 2 million. The effects of wing height on lift and pitching moment were small at most Mach numbers. The effect of Mach number on the inflection lift coefficients and the lift-curve and pitching-moment-curve slopes of the two configurations are shown in figures 6 and 7, respectively. The variation of these parameters with Mach number was generally similar for both wing positions; however, the low-wing configuration had slightly lower inflection lift coefficients except at Mach numbers near critical speed. At a lift coefficient of 0.40 the low-wing configuration was slightly more stable than the high-wing configuration at most Mach numbers.

The drag characteristics of the low-wing and high-wing configurations are compared for several Mach numbers in figures 5(b) and 5(d). At the lower lift coefficients, less drag was indicated for the high wing than for the low wing. The differences in drag increased with increasing Mach number. This effect is best shown by the data in figures 8 and 9 which show the variations with Mach number of drag coefficient for several constant lift coefficients and the maximum lift-drag ratio. The data in figure 8 show that the Mach numbers for drag divergence (defined at $(dC_D/dM)=0.10$) are somewhat lower for the low wing than for the high wing. The Mach numbers for drag divergence with their corresponding drag coefficients are compared for the two wing positions in the following table:

		C_L					
		0.10	0.20	0.30	0.40	0.50	0.60
Low wing	M for drag divergence	0.90	0.91	0.871	0.854	0.820	0.794
	C_D (at $(dC_D/dM) = 0.10$)	.0200	.0232	.0236	.0269	.0310	.0388
High wing	M for drag divergence	- - -		.892	.866	.846	.801
	C_D (at $(dC_D/dM) = 0.10$)	- - -		.0219	.0258	.0321	.0381

It should be pointed out that no attempt was made to improve the drag characteristics by use of fillets at the wing-fuselage juncture. A modification of this kind would probably be more beneficial to the low-wing configuration than to the high-wing configuration.

Wing-Fuselage-Tail Combinations

Longitudinal characteristics with a horizontal tail.- The longitudinal characteristics of the wing-fuselage-tail combination having the low wing are presented in figures 10 through 13 for several tail heights and angles of incidence. These figures also show the wing-fuselage data of figures 3 and 5. Generally, the addition of the tail resulted in small increases in lift-curve slope and drag; these were of approximately the same magnitude as those shown for the high-wing configuration (ref. 2). The inflection lift coefficients were generally higher with the tail on than with it off. Figure 14 compares the variation of inflection lift coefficient with Mach number for the low- and high-wing combinations with a horizontal tail. These variations were generally similar for both wing positions, and show that usually the low-wing combination had lower inflection lift coefficients than the high-wing configuration.

The factors which determine the tail contribution to the stability are shown in figure 15 as a function of angle of attack for several Mach numbers, Reynolds numbers, and horizontal-tail heights. The method used to calculate the effective downwash angle ϵ, the tail efficiency factor $\eta_t(q_t/q)$, and the ratio of the lift-curve slope of the isolated tail to the lift-curve slope of the wing-fuselage combination a_t/a_{w+f}, was the same as that of reference 2. The wing-fuselage force data presented in figures 3 and 5 and the isolated tail data of reference 2 were used for these computations. These results show that the improvement in the pitching-moment characteristics at the higher lift coefficients due to adding the tail were mostly a result of an increase in the factor a_t/a_{w+f} with increasing lift coefficient in a manner which offset the reduction in stability of the wing-fuselage combination at high lift. This was generally true at all Mach numbers. The variations with Mach number of

the various factors affecting the stability contribution of the horizontal tail and the variation of the tail-control effectiveness parameter $\partial C_m/\partial i_t$ are compared at an angle of attack of 4° in figures 16 and 17 with data from reference 2 for the high-wing configuration.

Effects of tail height.- The pitching-moment characteristics for several tail heights at several Mach numbers are presented in figure 18. Raising the tail of the low-wing combination above the fuselage center line (0.13 b/2) generally increased slightly the longitudinal stability and the lift coefficient for balance. The effect of raising the tail on the factors affecting the stability contribution of the tail is shown in figure 15. Raising the tail resulted in increases in the rate of change of downwash with angle of attack; however, this destabilizing effect of increased tail height was more than compensated for by increases in tail efficiency factor $\eta_t(q_t/q)$. Figure 17, which shows the tail-control effectiveness parameter $\partial C_m/\partial i_t$ as a function of Mach number, indicates that for the low wing at a Mach number of 0.80 an improvement of about 60 percent in tail-control effectiveness resulted from raising the horizontal tail from the fuselage center line (0.13 b/2) to a position above the center line (0.20 b/2). Further increases in tail height resulted in no significant changes in the control effectiveness. Figure 17 also shows that the horizontal tail on the fuselage center line (0.13 b/2) of the low-wing configuration was a less effective longitudinal control than the tail on the fuselage center line (0 b/2) of the high-wing configuration by about 37 percent at a Mach number of 0.25 and by about 9 percent at a Mach number of 0.90. These differences were due mostly to the adverse effect of lowering the wing on the dynamic pressure at the tail resulting from wing-fuselage interference. The tail-control effectiveness was nearly the same for both the low- and high-wing combinations with the horizontal tail above the plane of the wing root chord.

CONCLUSIONS

A wind-tunnel investigation has been made of a low-wing, wing-fuselage combination with and without a horizontal tail. The wing had camber, twist, 40° of sweepback, and fences on the upper surface. The results of the investigation are compared with those of a previous investigation with the wing mounted high on the fuselage. The following conclusions are indicated:

1. The effects of wing height were small; although the low-wing configuration had generally higher drags and lower drag-divergence Mach numbers than the high-wing configuration.

2. The low-wing configuration had slightly lower lift-curve slopes but greater lift near zero angle of attack than did the high-wing configuration.

3. Raising the horizontal tail of the low-wing configuration generally increased the longitudinal stability and the lift coefficient for balance. Raising the tail 0.07 b/2 above the fuselage center line resulted in an increase of about 60 percent in the effectiveness of the horizontal tail as a longitudinal control at a Mach number of 0.80. Further increases in tail height had only small effect on the control effectiveness.

4. When mounted on the fuselage center line, the horizontal tail of the low-wing configuration was less effective as a longitudinal control by about 37 percent at 0.25 Mach number and by about 9 percent at 0.90 Mach number than when mounted on the fuselage center line of the high-wing configuration; however, the tail-control effectiveness was nearly the same for both configurations with the tail above the fuselage center line.

Ames Aeronautical Laboratory
National Advisory Committee for Aeronautics
Moffett Field, Calif., March 30, 1955

REFERENCES

1. Sutton, Fred B., and Dickson, Jerald K.: A Comparison of the Longitudinal Aerodynamic Characteristics at Mach Numbers up to 0.94 of Sweptback Wings Having NACA 4-Digit or NACA 64A Thickness Distributions. NACA RM A54F18, 1954.

2. Sutton, Fred B., and Dickson, Jerald K.: The Longitudinal Characteristics at Mach Numbers up to 0.92 of Several Wing-Fuselage-Tail Combinations Having Sweptback Wings With Four-Digit Thickness Distributions. NACA RM A54L08, 1955.

3. Herriot, John G.: Blockage Corrections for Three-Dimensional-Flow Closed-Throat Wind Tunnels, With Consideration of the Effect of Compressibility. NACA Rep. 995, 1950. (Formerly NACA RM A7B28.)

4. Sivells, James C., and Salmi, Rachel M.: Jet-Boundary Corrections for Complete and Semispan Swept Wings in Closed Circular Wind Tunnels. NACA TN 2454, 1951.

5. Schlichting, H.: Report on the Special Field "Interference" to the Wind-Tunnel Committee in February 1945. NACA TM 1347, 1953.

TABLE I.- FUSELAGE COORDINATES

Distance from nose, in.	Radius, in.
0	0
1.27	1.04
2.54	1.57
5.08	2.35
10.16	3.36
20.31	4.44
30.47	4.90
39.44	5.00
50.00	5.00
60.00	5.00
70.00	5.00
76.00	4.96
82.00	4.83
88.00	4.61
94.00	4.27
100.00	3.77
106.00	3.03
126.00	0

TABLE II.- CORRECTIONS TO DATA

(a) Corrections for constriction effects

Corrected Mach number	Uncorrected Mach number	$\frac{q_{corrected}}{q_{uncorrected}}$
0.25	0.250	1.003
.60	.599	1.006
.70	.696	1.007
.80	.793	1.010
.83	.821	1.012
.86	.848	1.015
.88	.866	1.017
.90	.883	1.020
.92	.899	1.024

(b) Corrections for tunnel-wall interference

$\Delta\alpha = 0.455C_L$

$\Delta C_D = 0.00662{C_L}^2$

$\Delta C_{m_{tail\ off}} = K_1 C_{L_{tail\ off}}$

$$\Delta C_{m_{tail\ on}} = K_1 C_{L_{tail\ off}} - \left[(K_2 C_{L_{tail\ on}} - \Delta\alpha)\frac{\partial C_m}{\partial i_t}\right]$$

where:

Mach number	K_1	K_2
0.25	0.0027	0.72
.60	.0038	.74
.70	.0043	.76
.80	.0049	.79
.83	.0050	.80
.86	.0053	.83
.88	.0054	.84
.90	.0056	.86
.92	.0057	.88

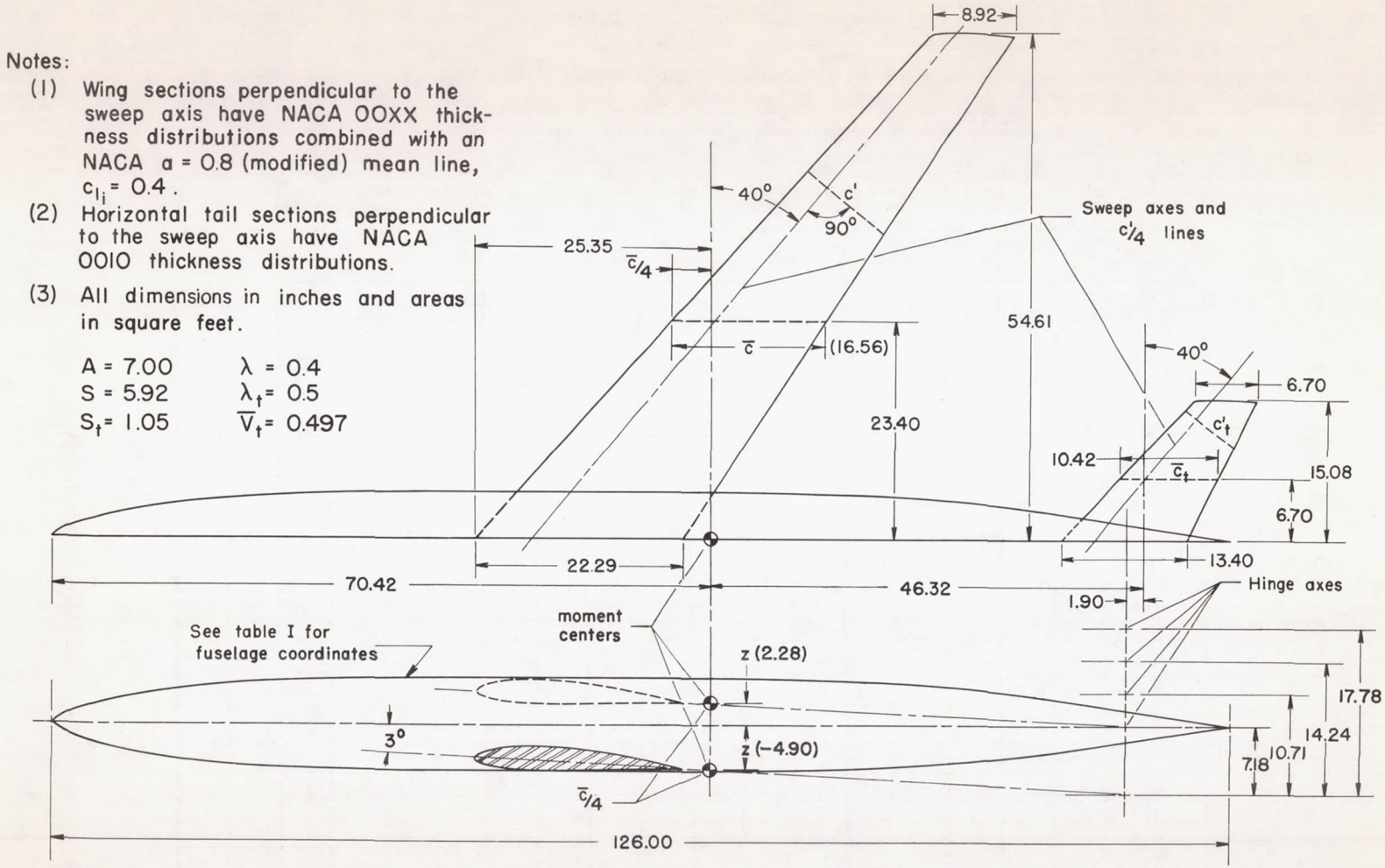

(a) Model dimensions.

Figure 1.- Geometry of the model.

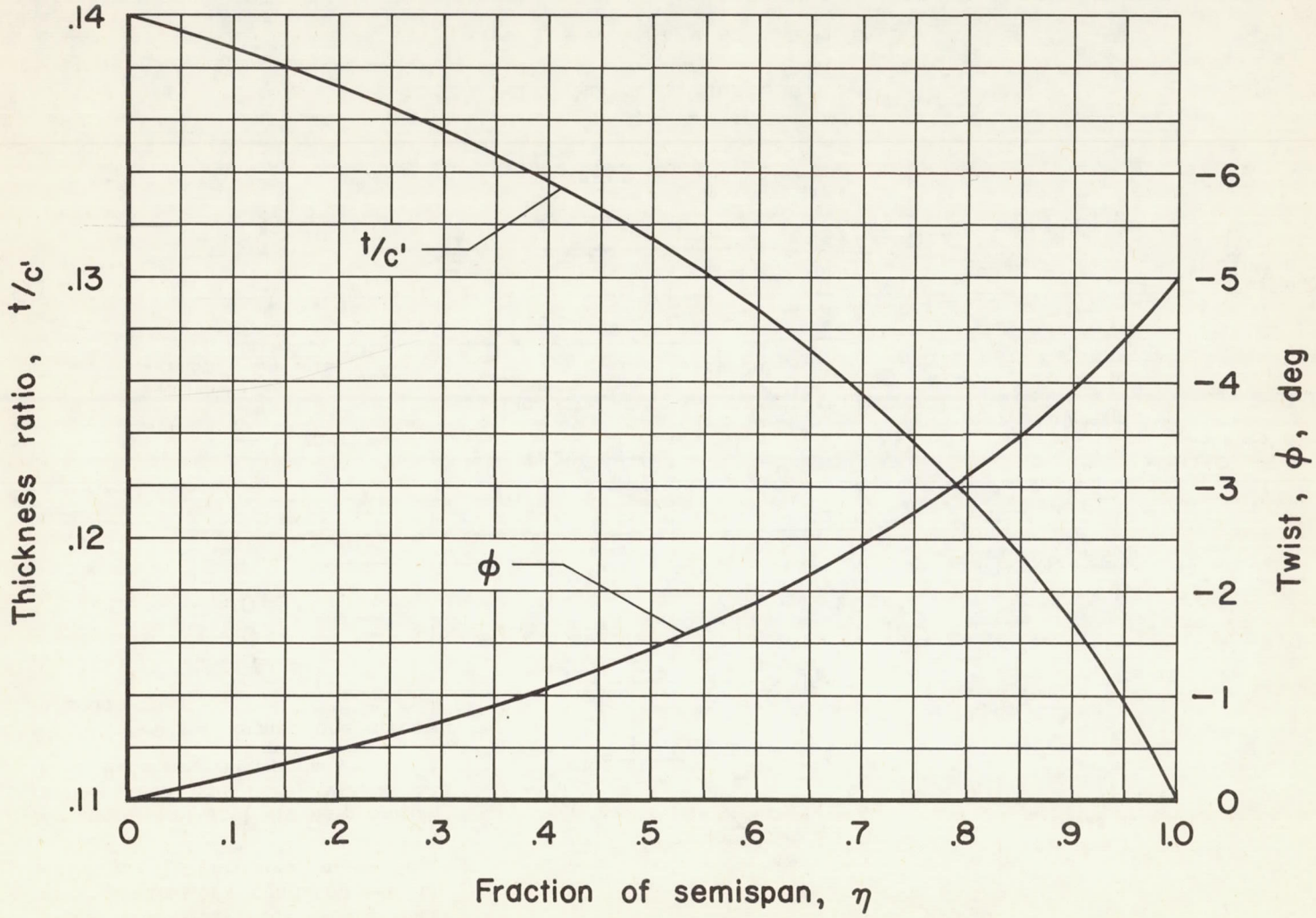

(b) Thickness ratio and twist distribution.

Figure 1.- Continued.

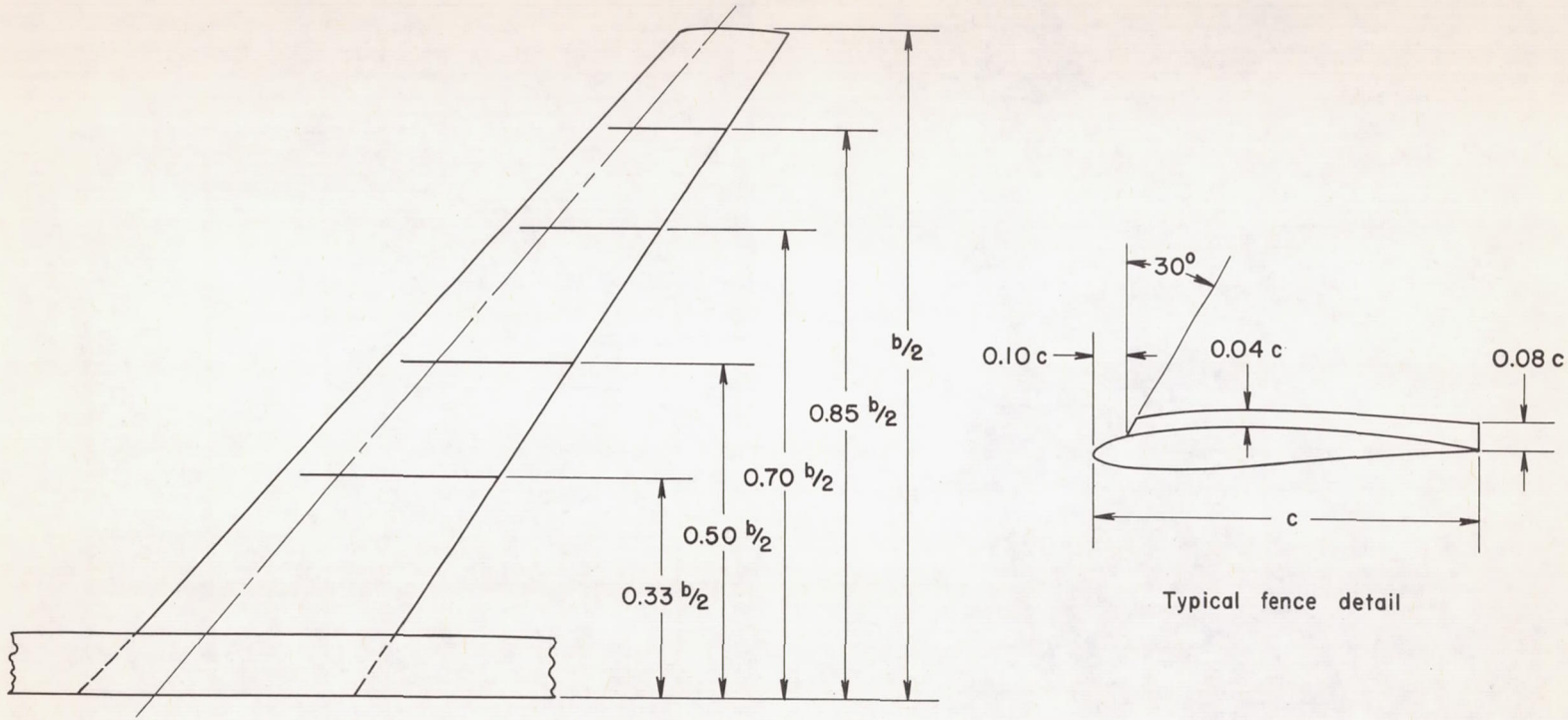

(c) Fence details and locations.

Figure 1.- Concluded.

(a) Low-wing model. A-19571

(b) High-wing model. A-19214

Figure 2.- Photographs of the models.

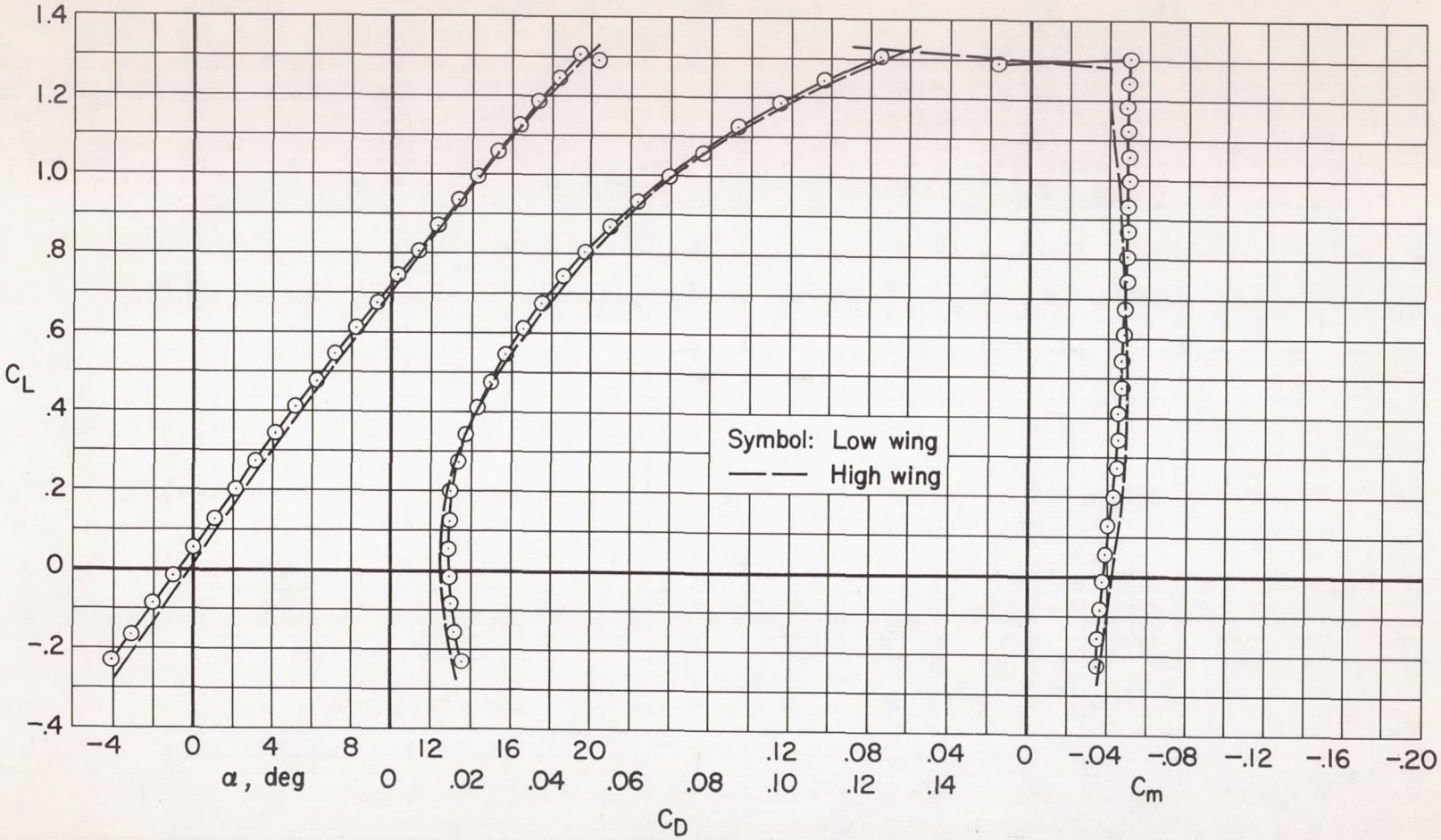

Figure 3.- The effect of wing height on the longitudinal characteristics of the wing-fuselage combinations at low speed; M = 0.25, R = 8,000,000.

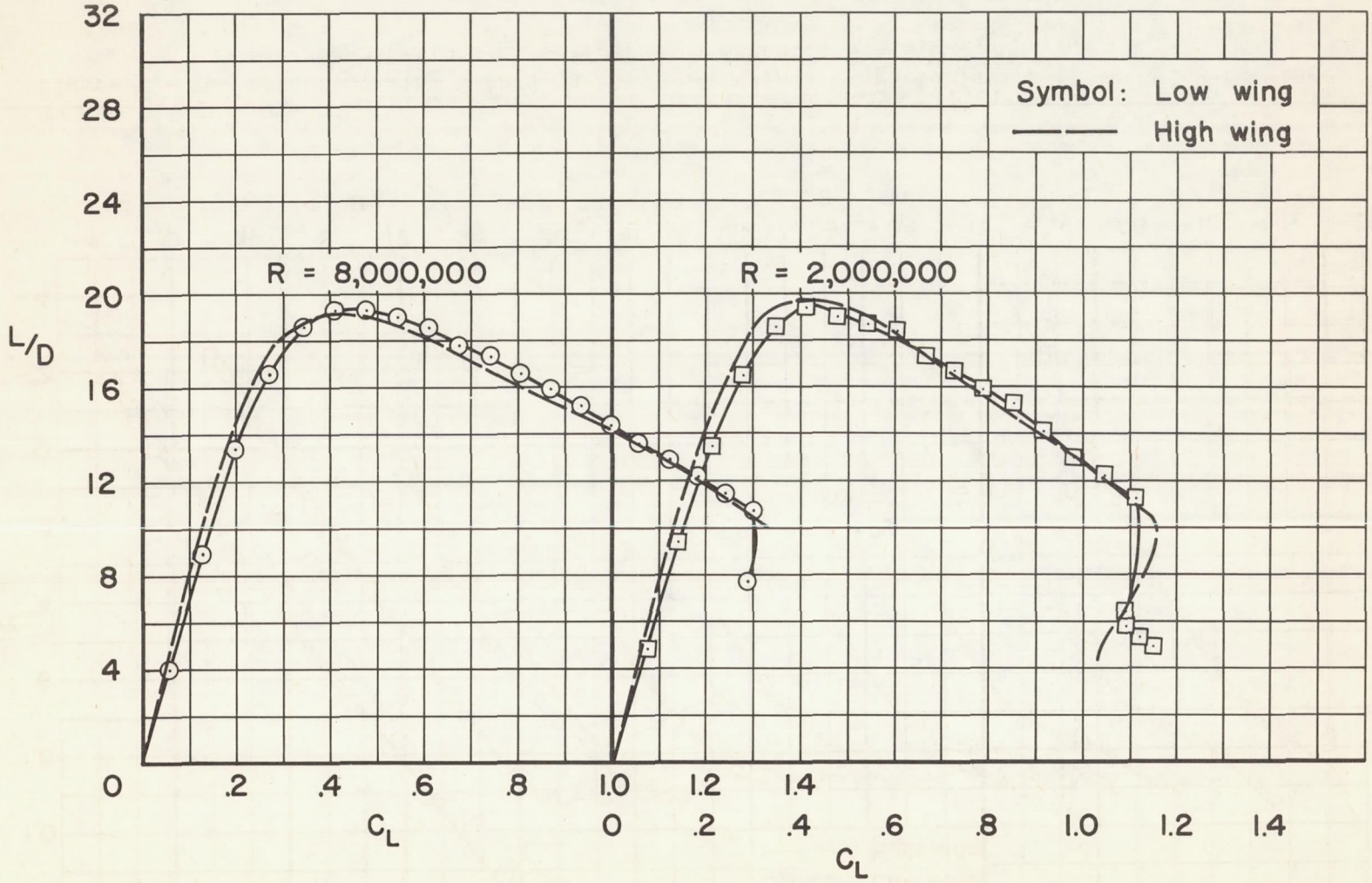

Figure 4.- The effect of wing height and Reynolds number on the lift-drag ratio of the wing-fuselage combinations at low speed; M = 0.25.

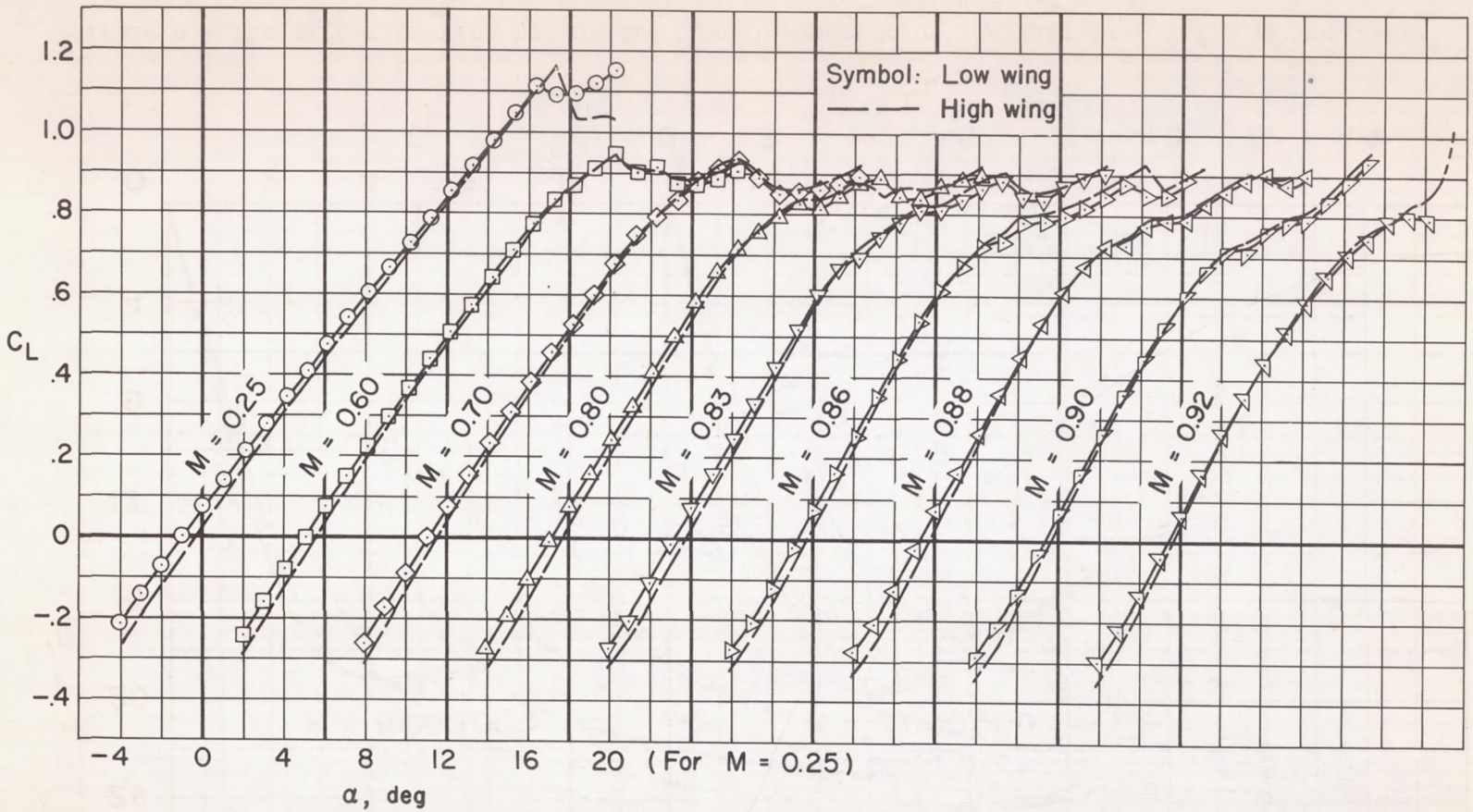

(a) C_L vs. α

Figure 5.- The effect of wing height on the longitudinal characteristics of the wing-fuselage combinations at several Mach numbers; R = 2,000,000.

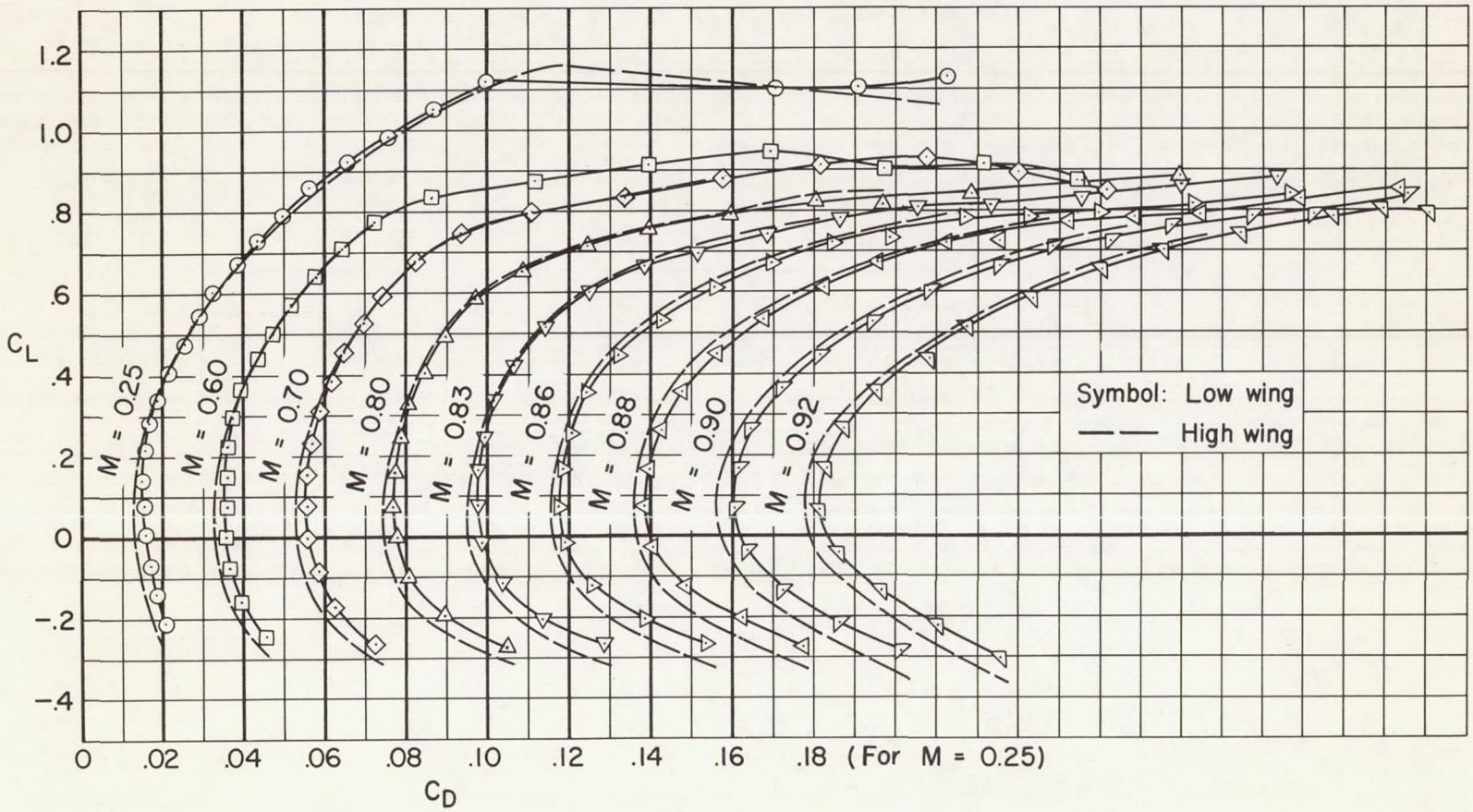

(b) C_L vs. C_D

Figure 5.- Continued.

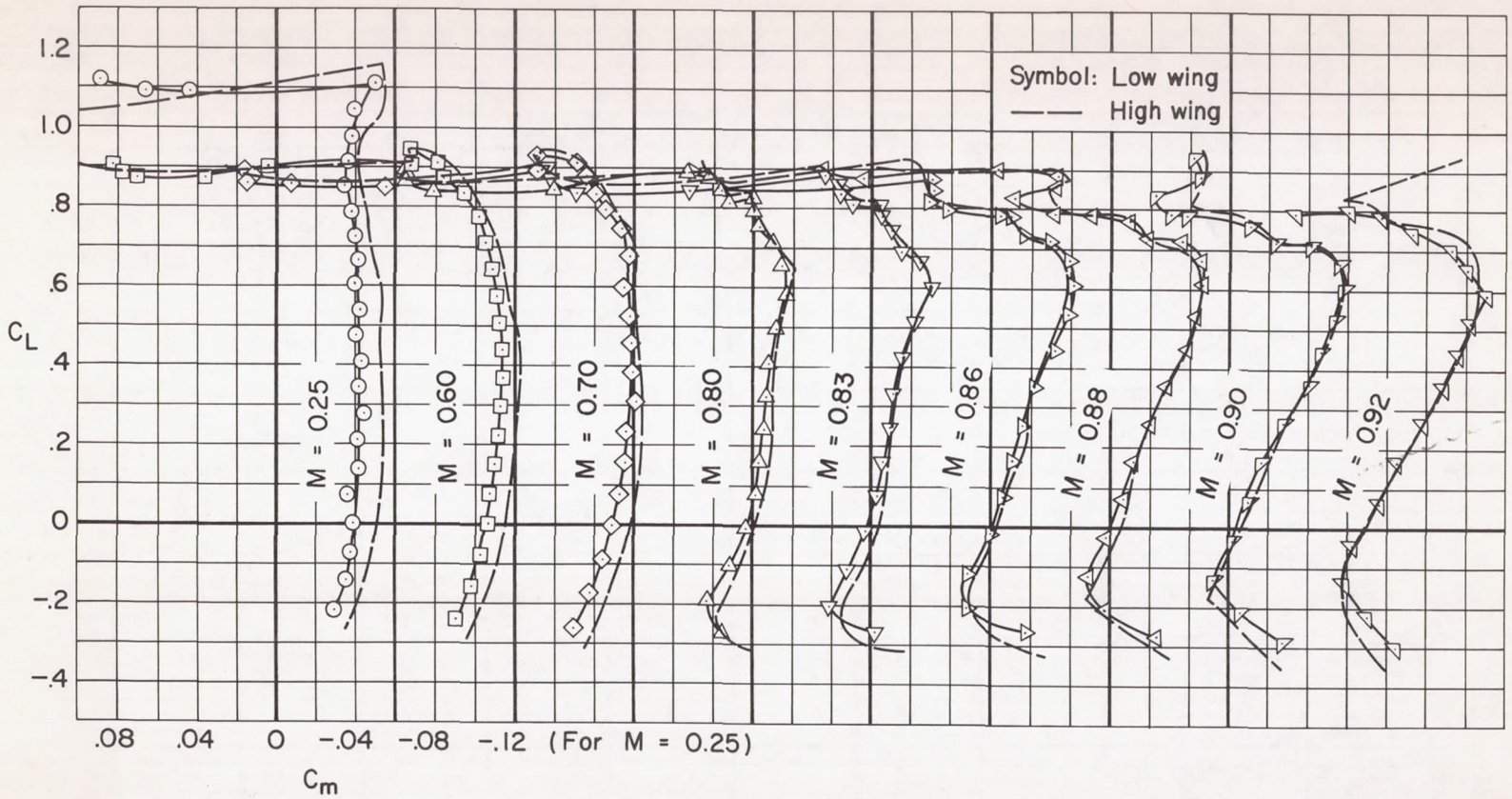

(c) C_L vs. C_m

Figure 5.- Continued.

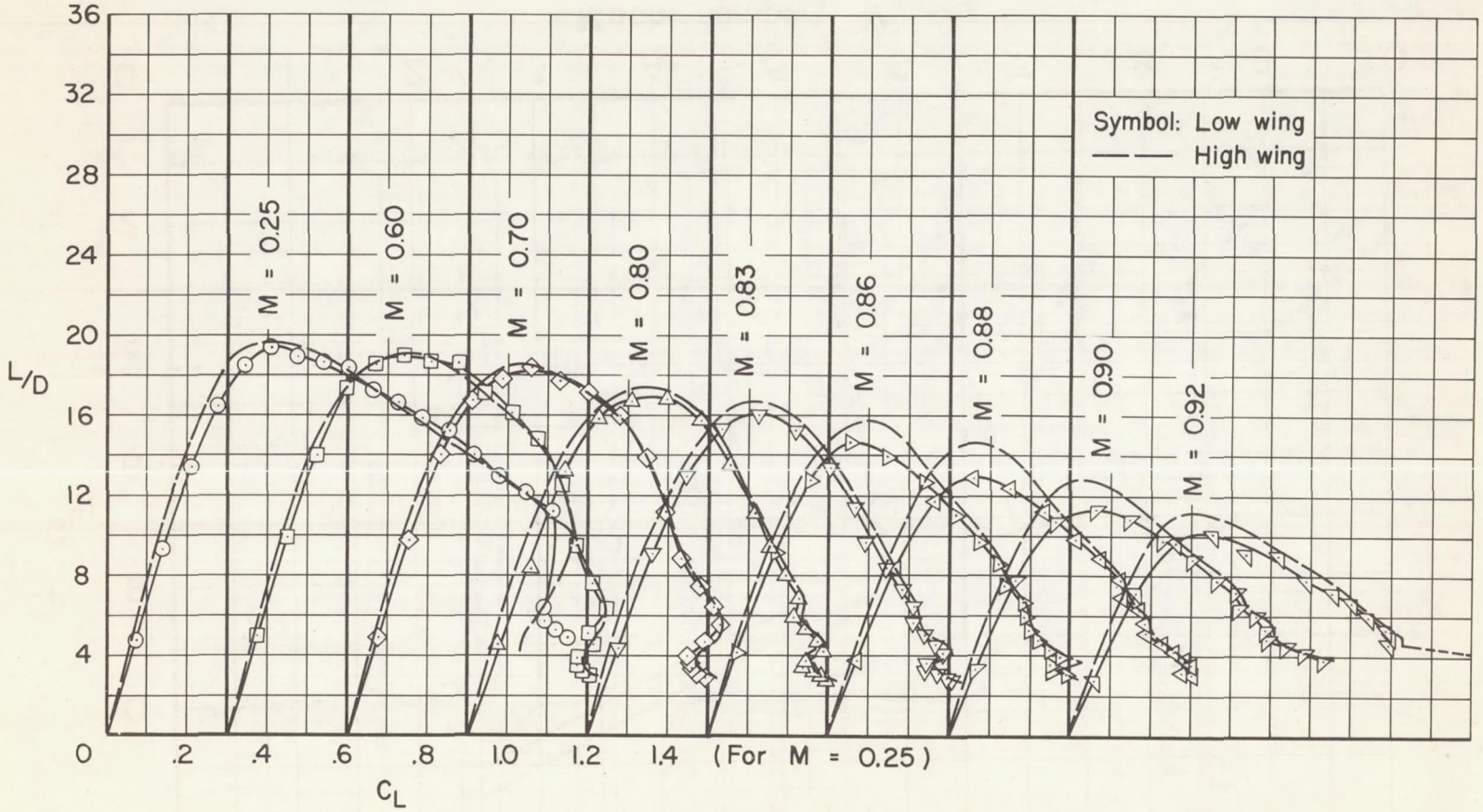

(d) L/D vs. C_L

Figure 5.- Concluded.

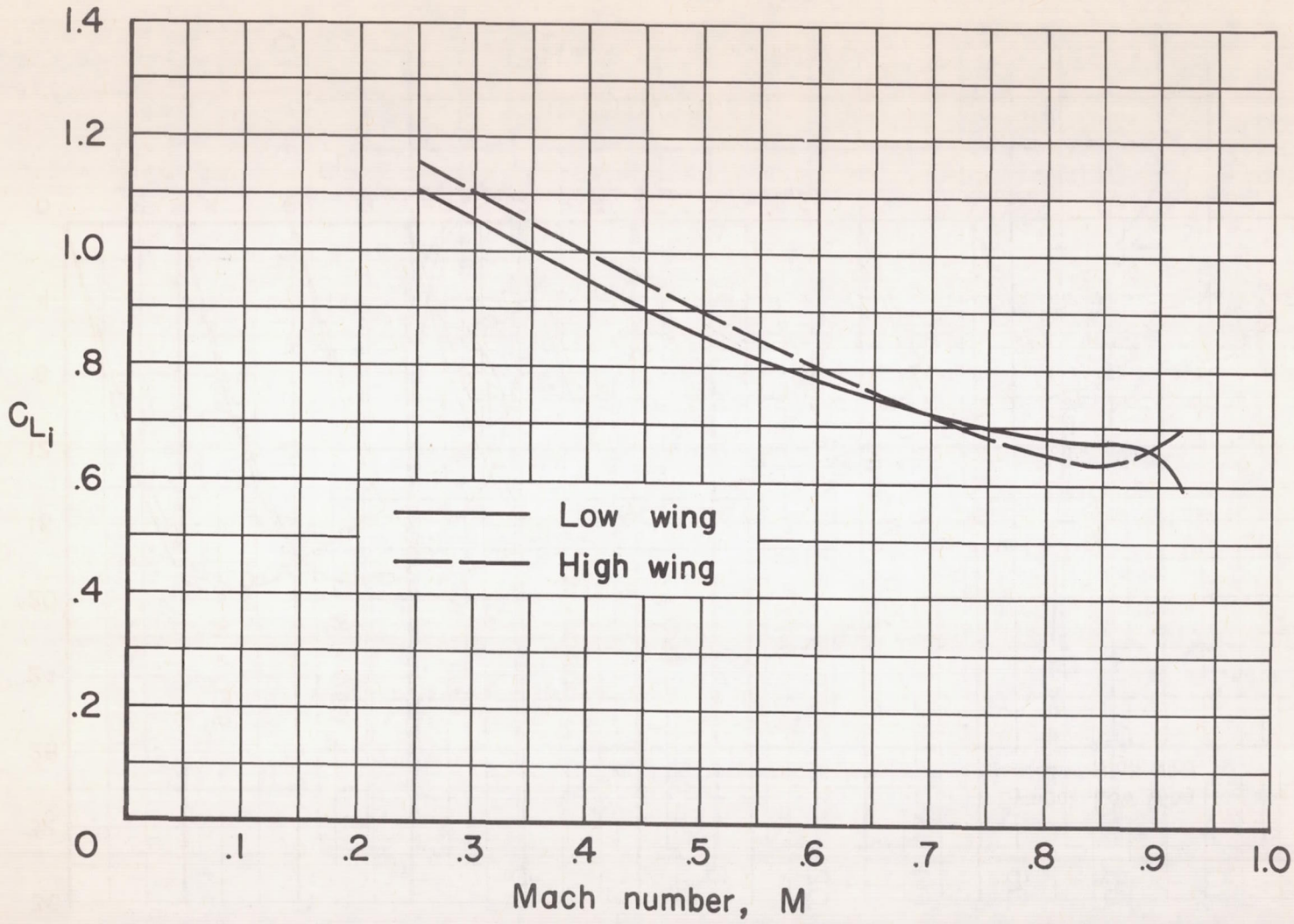

Figure 6.- The variation of inflection lift coefficient with Mach number for the low- and high-wing, wing-fuselage combinations; R = 2,000,000.

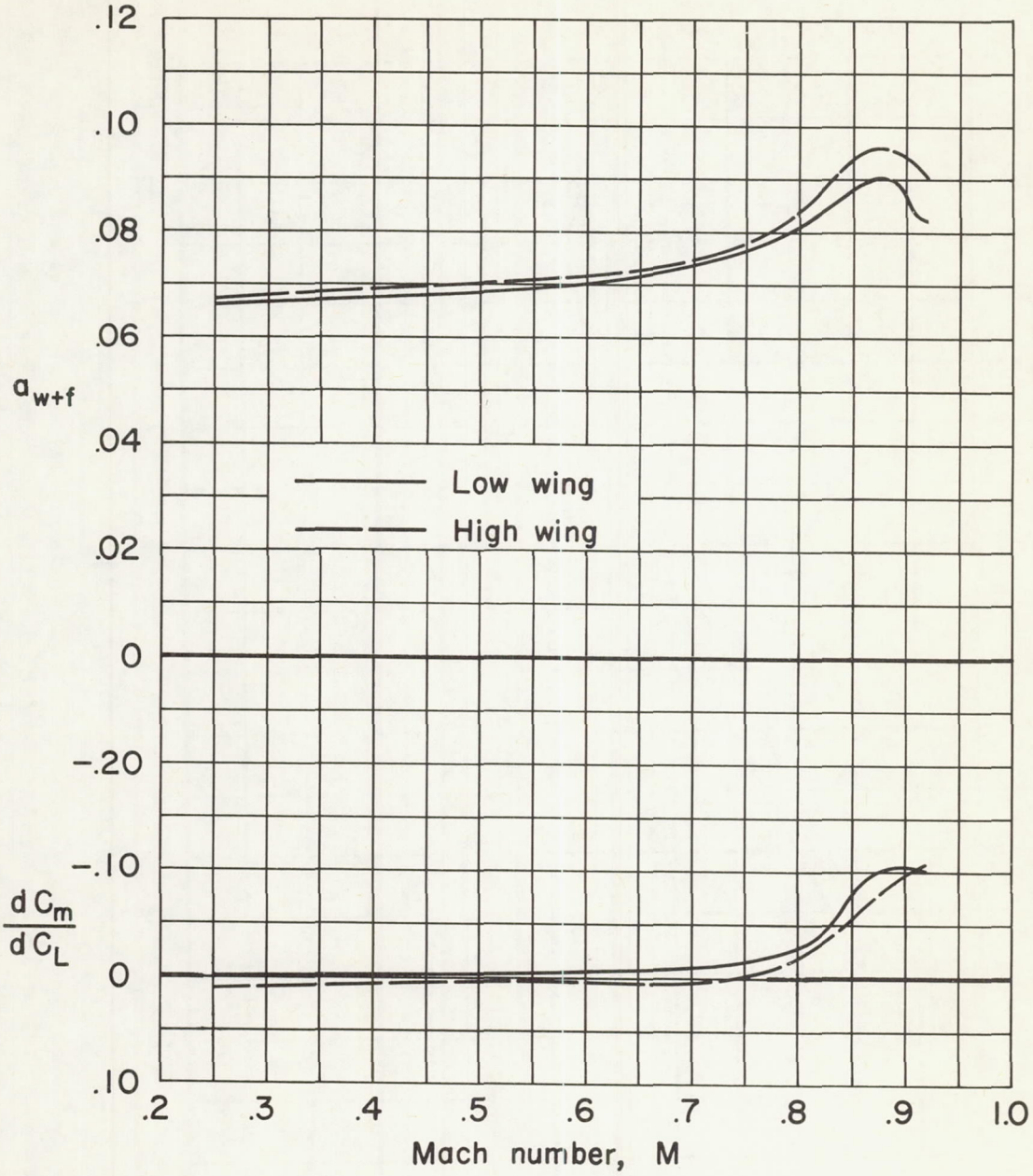

Figure 7.- The variation with Mach number of the lift-curve and pitching-moment-curve slopes of the low- and high-wing, wing-fuselage combinations; R = 2,000,000; C_L = 0.40.

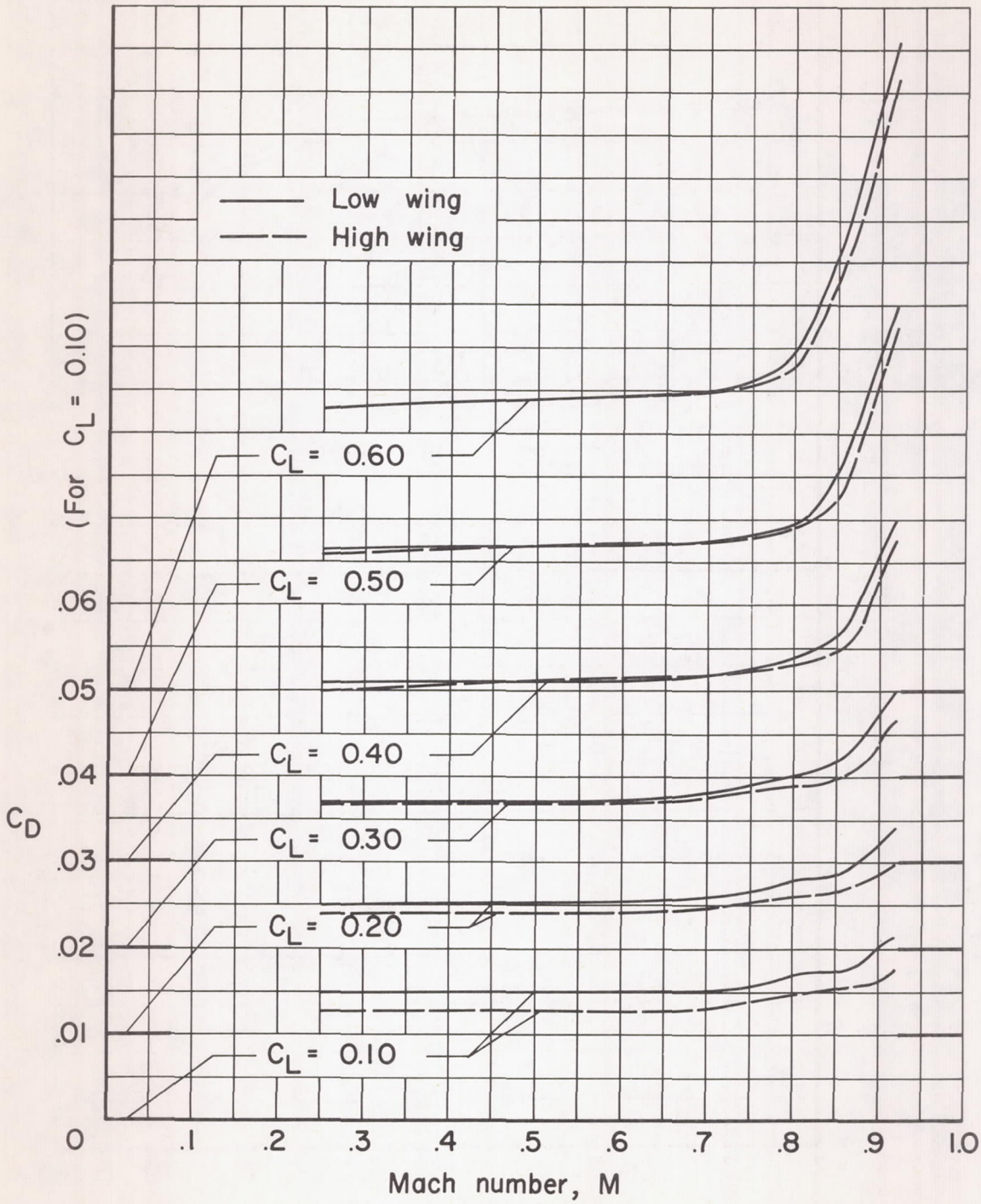

Figure 8.- The variation with Mach number of the drag characteristics of the low- and high-wing, wing-fuselage combinations at several constant lift coefficients; R = 2,000,000.

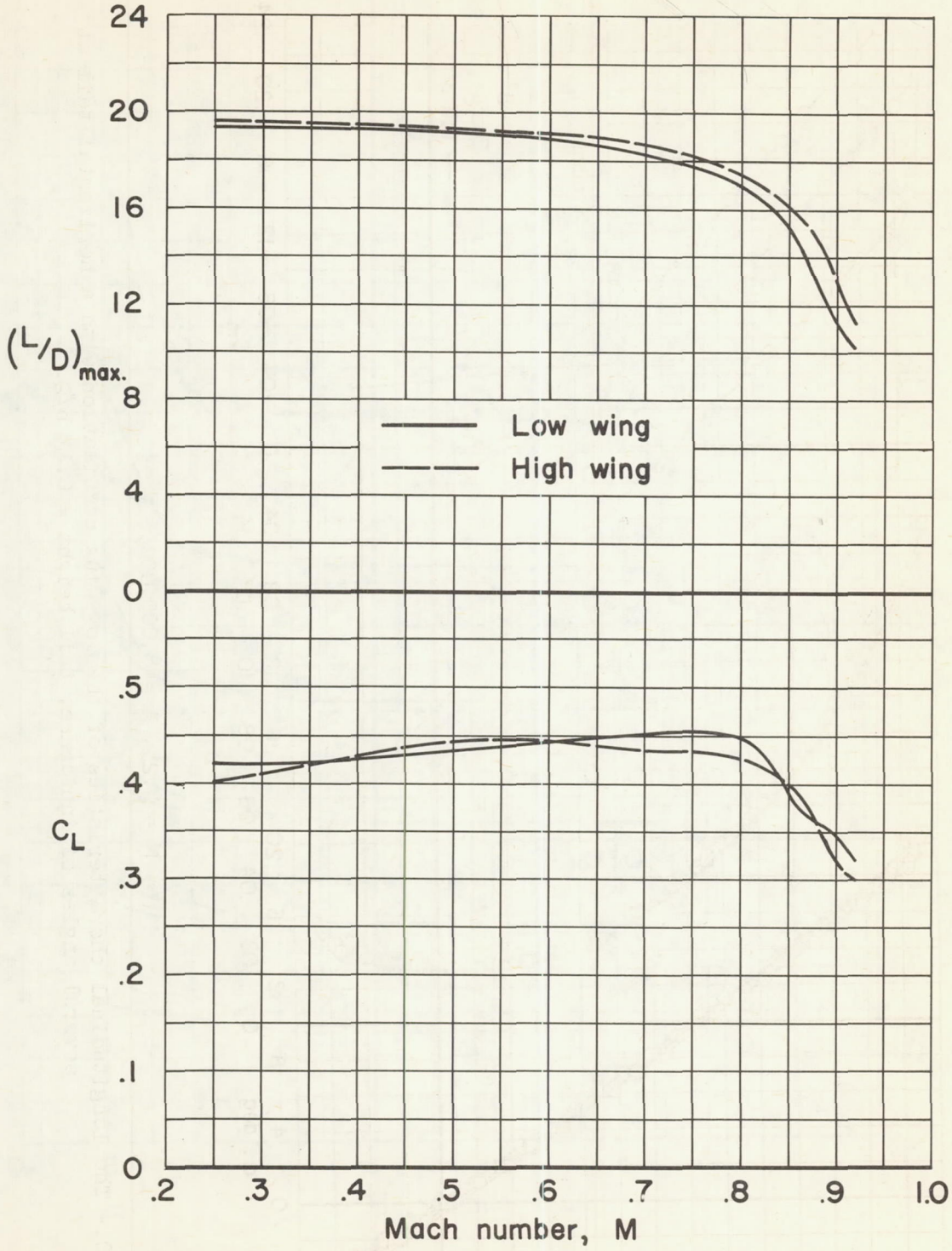

Figure 9.- The variation with Mach number of the maximum lift-drag ratio and lift coefficient for maximum lift-drag ratio of the low- and high-wing, wing-fuselage combinations; R = 2,000,000.

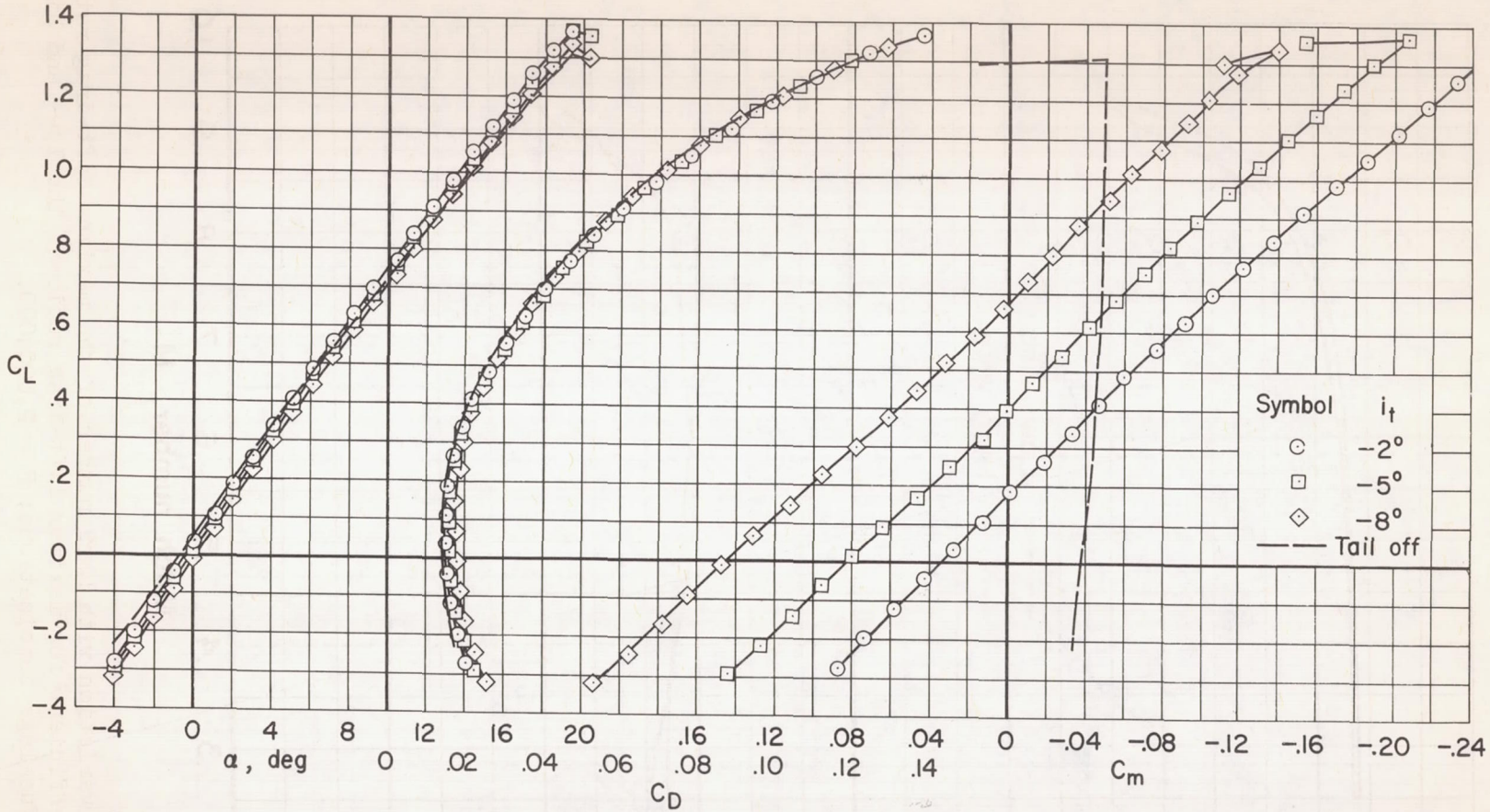

(a) M = 0.25, R = 8,000,000.

Figure 10.- The longitudinal characteristics of the low-wing combination with a horizontal tail at several angles of incidence; tail height = 0.13 b/2.

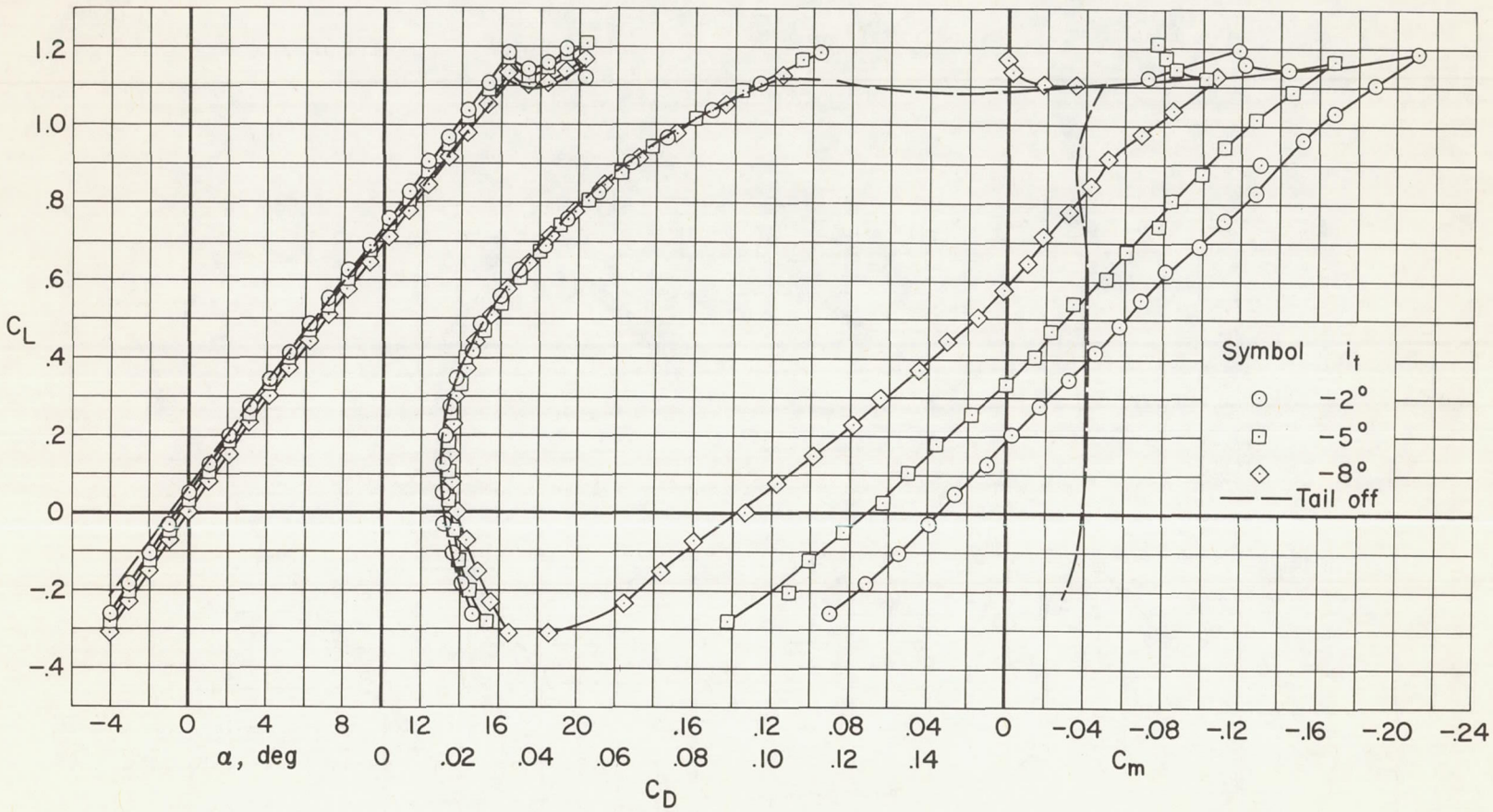

(b) M = 0.25, R = 2,000,000.

Figure 10.- Continued.

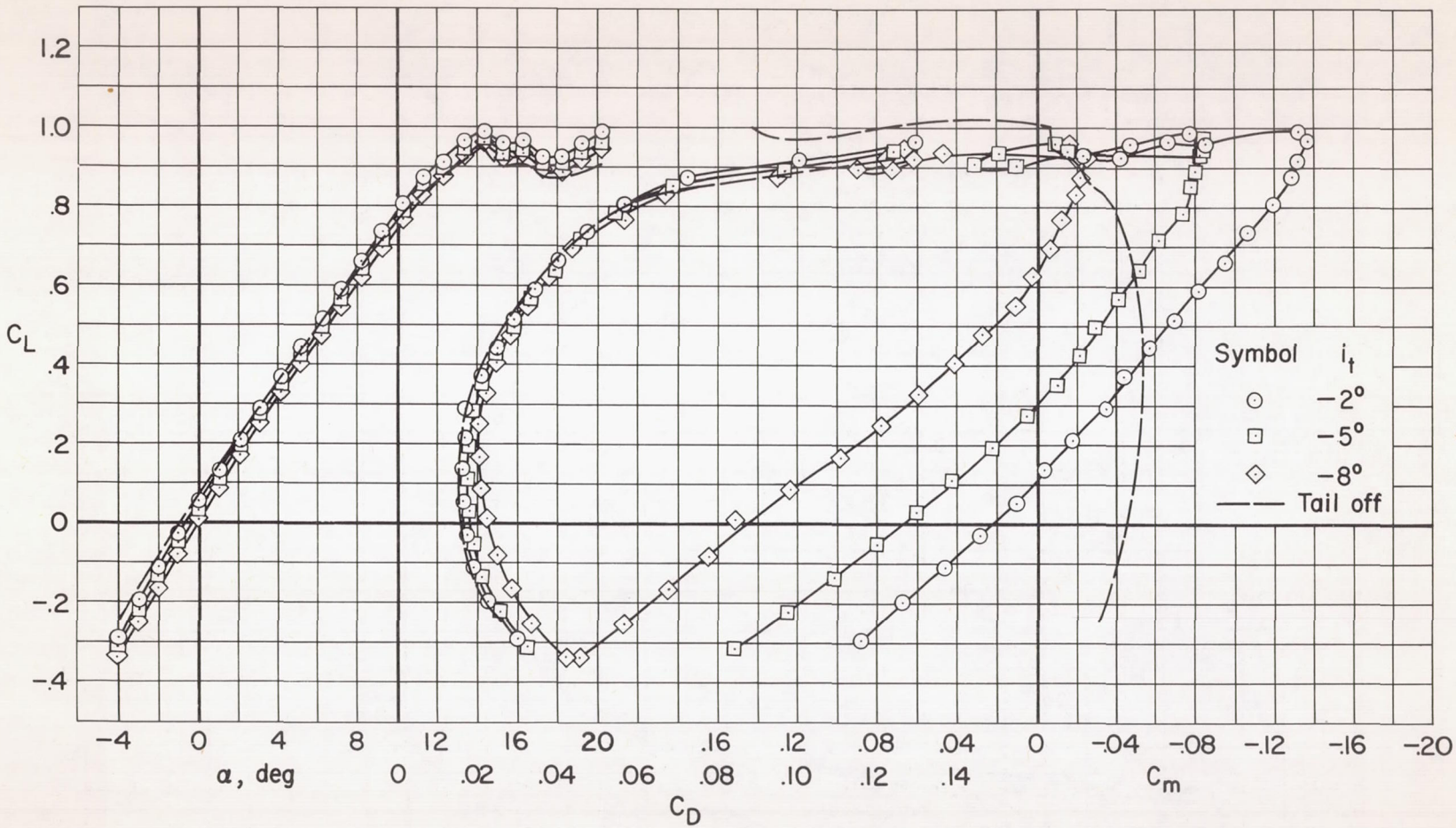

(c) M = 0.60, R = 2,000,000.

Figure 10.- Continued.

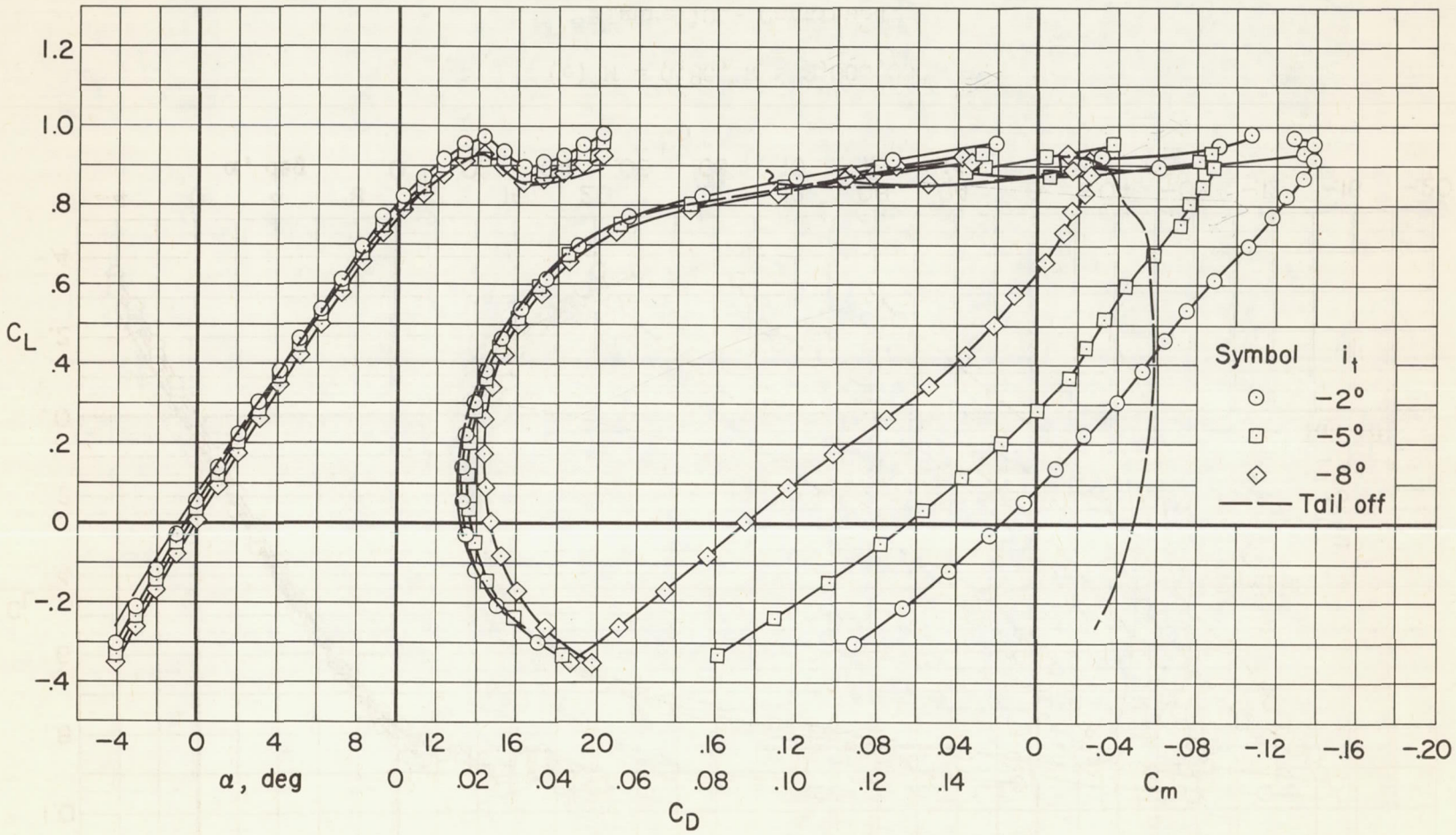

(d) M = 0.70, R = 2,000,000.

Figure 10.- Continued.

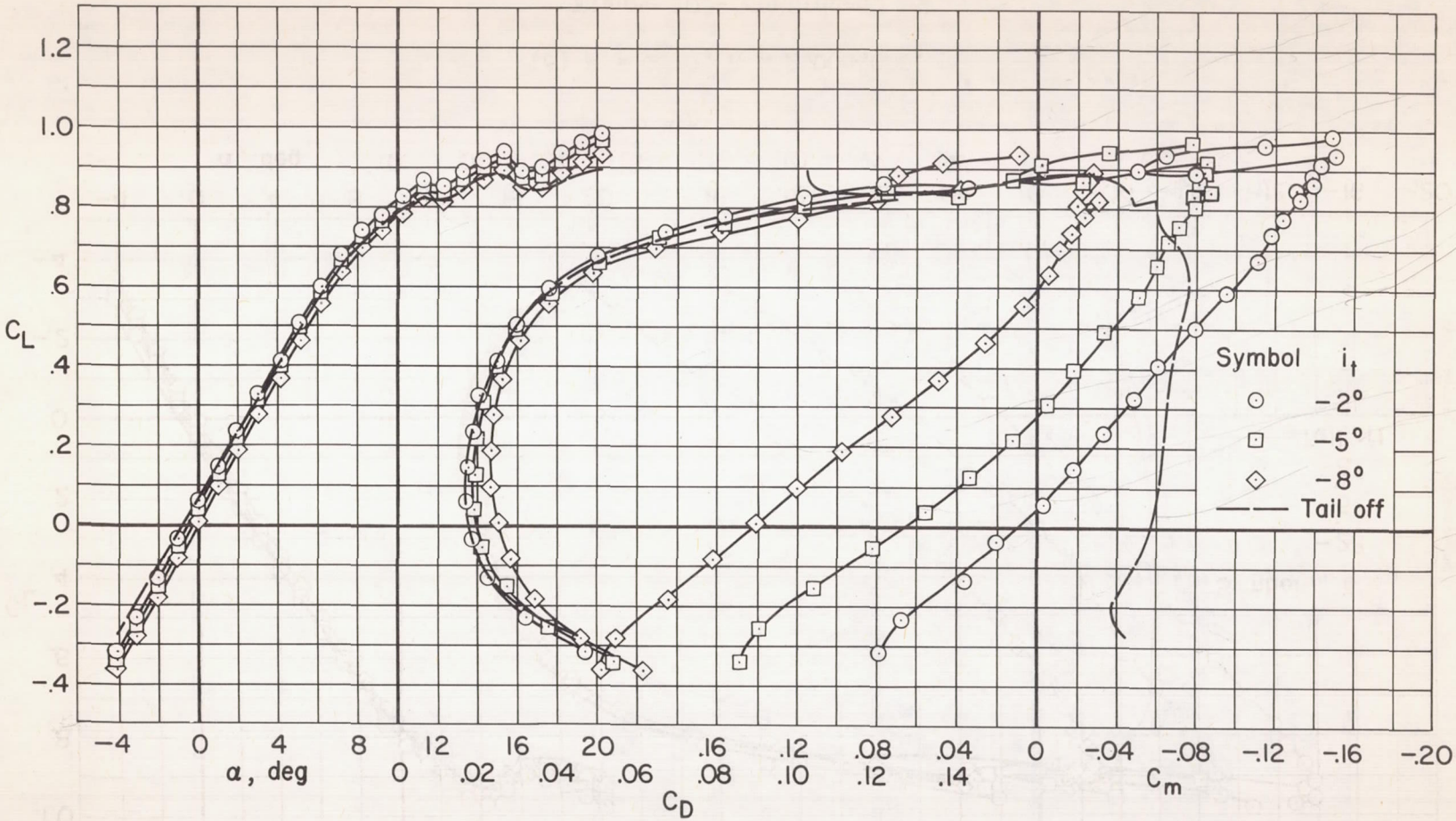

(e) M = 0.80, R = 2,000,000.

Figure 10.- Continued.

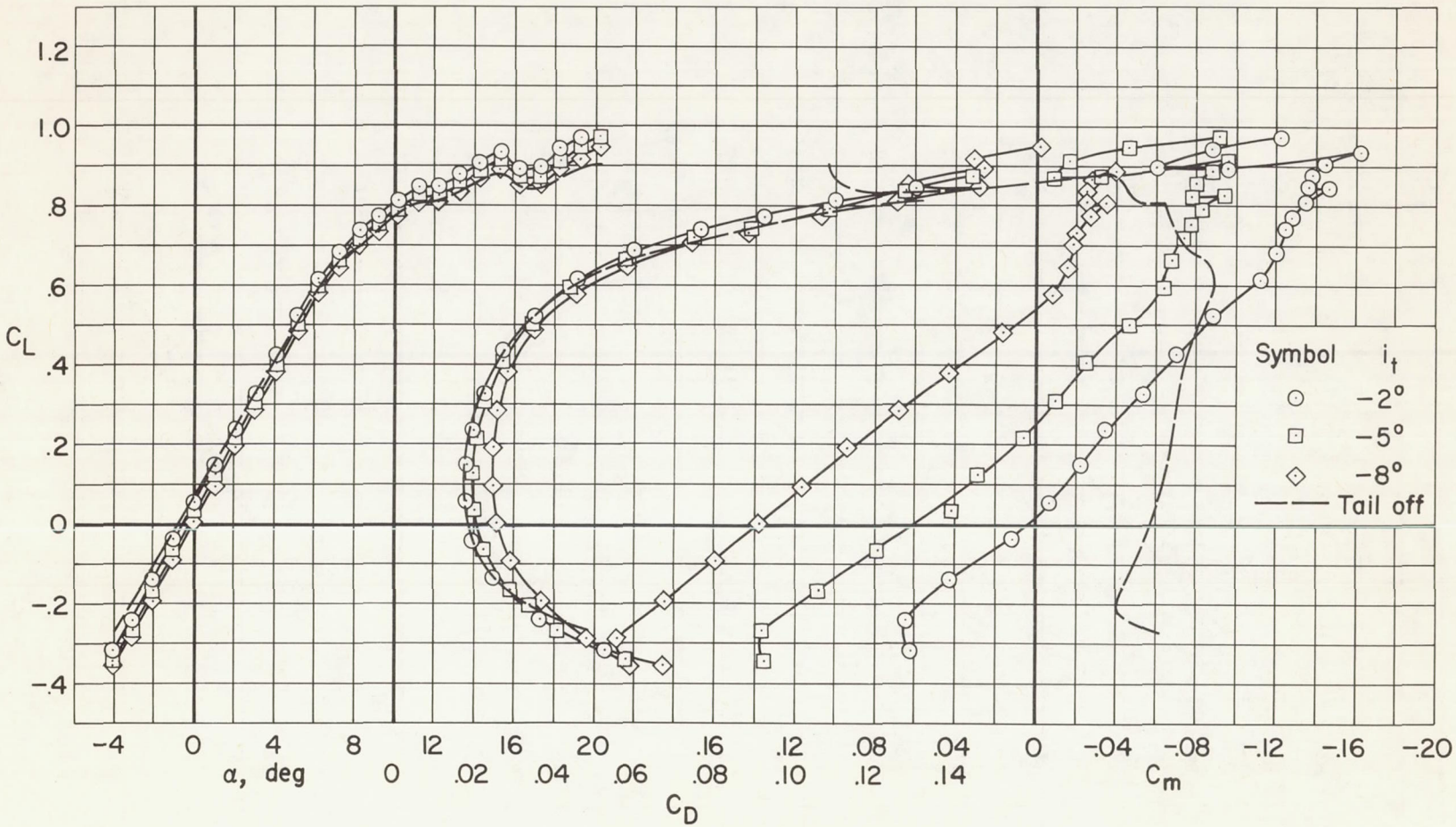

(f) M = 0.83, R = 2,000,000.

Figure 10.- Continued.

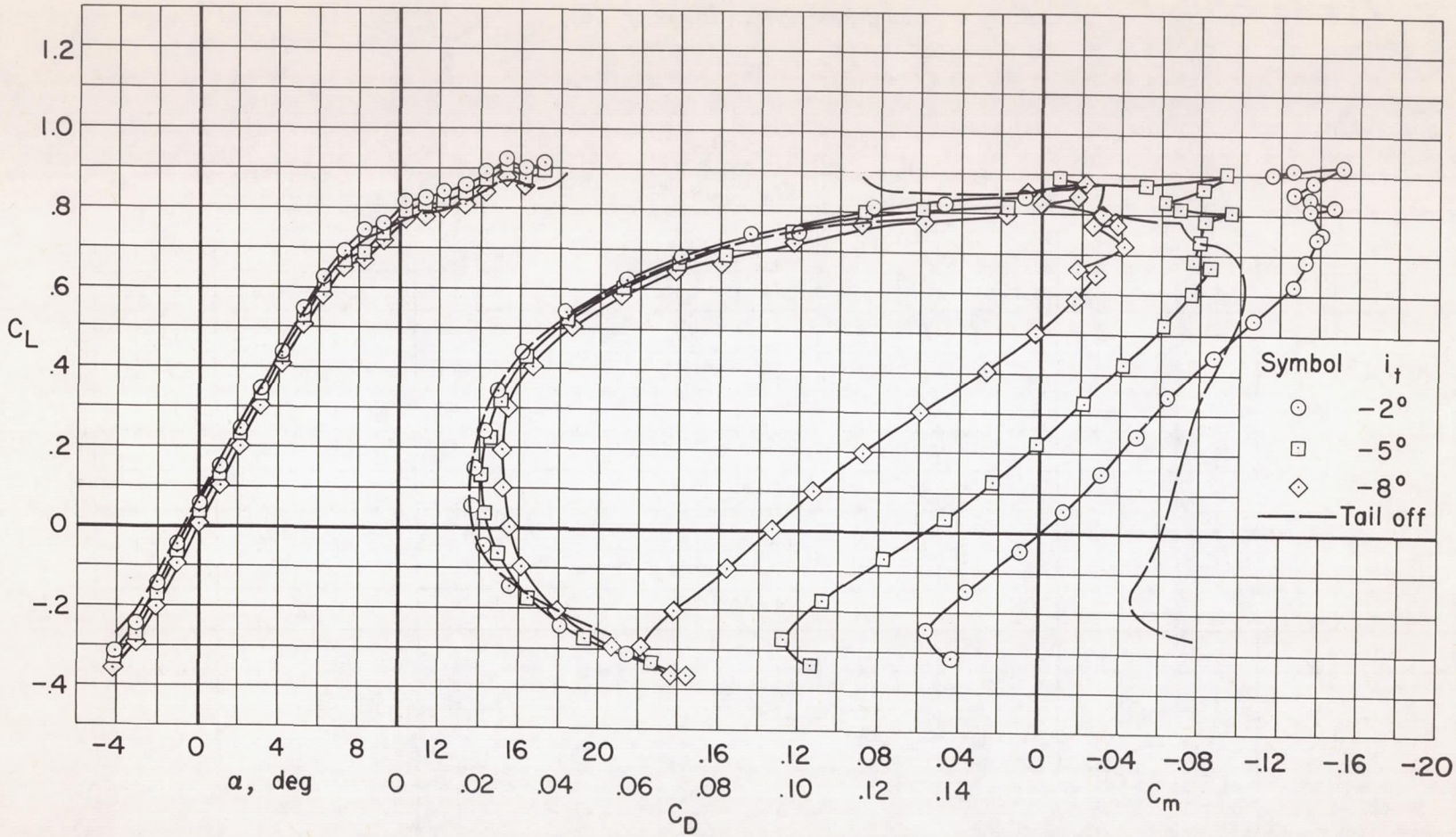

(g) M = 0.86, R = 2,000,000.

Figure 10.- Continued.

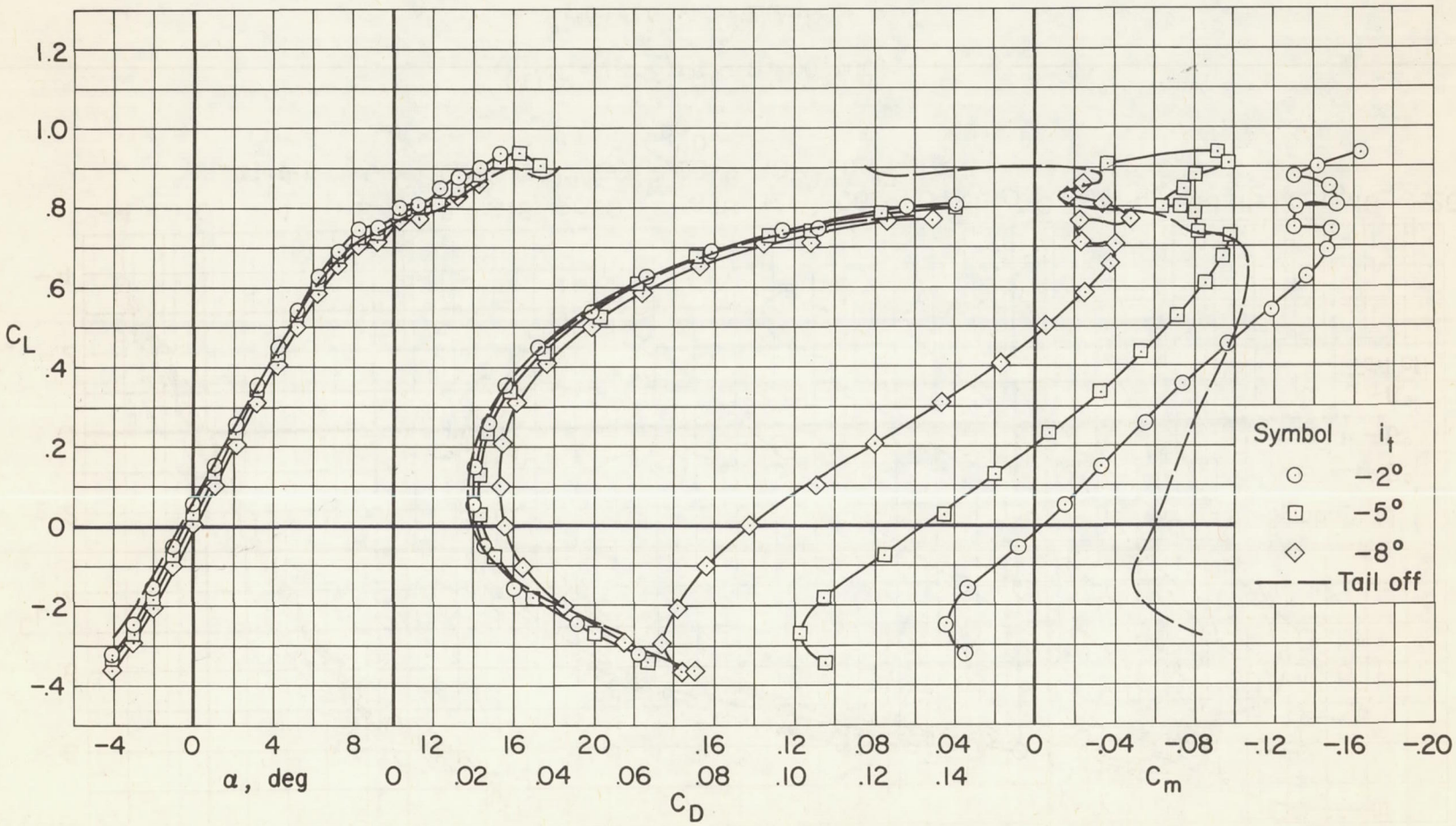

(h) M = 0.88, R = 2,000,000.

Figure 10.- Continued.

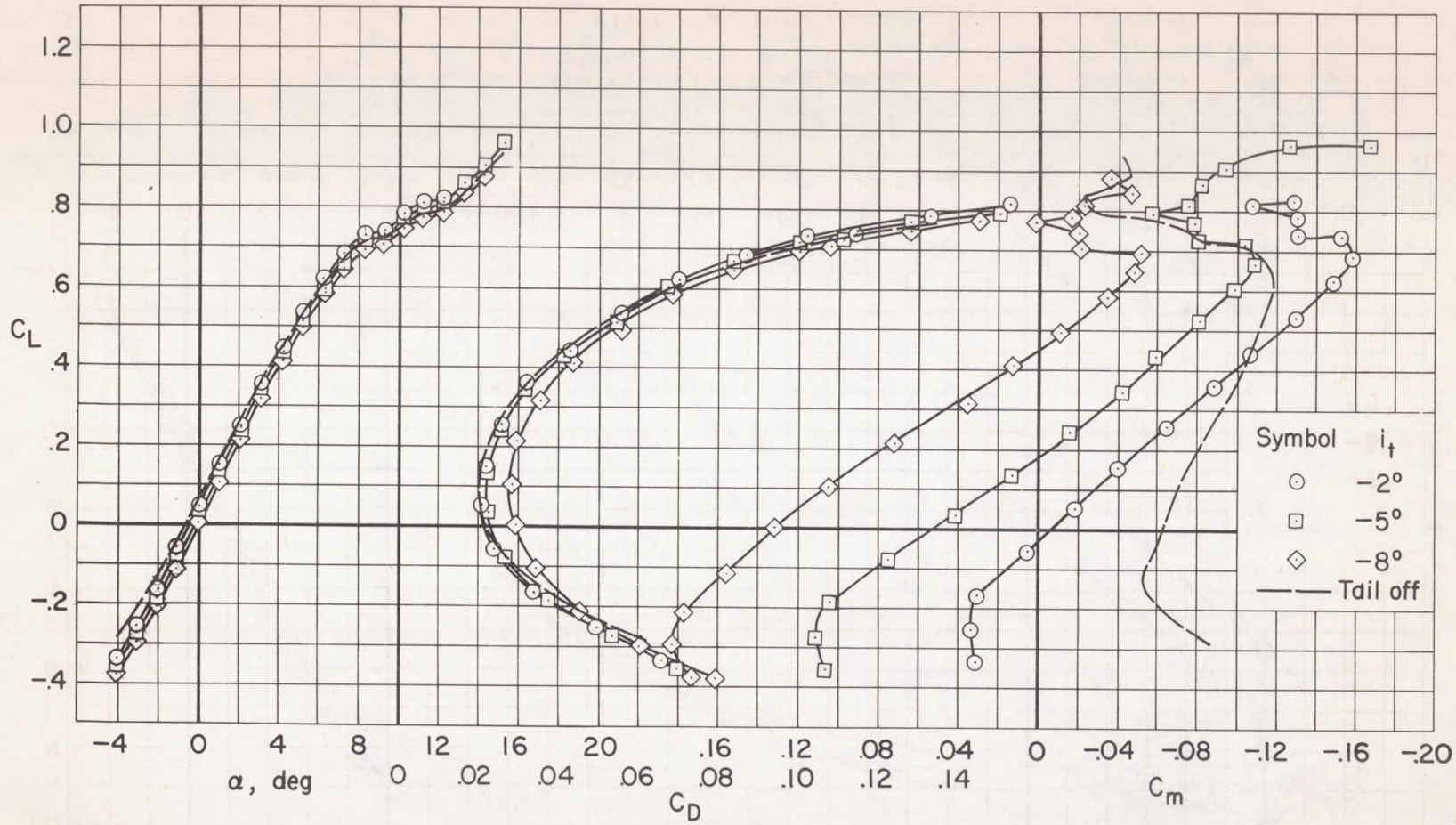

(i) M = 0.90, R = 2,000,000.

Figure 10.- Continued.

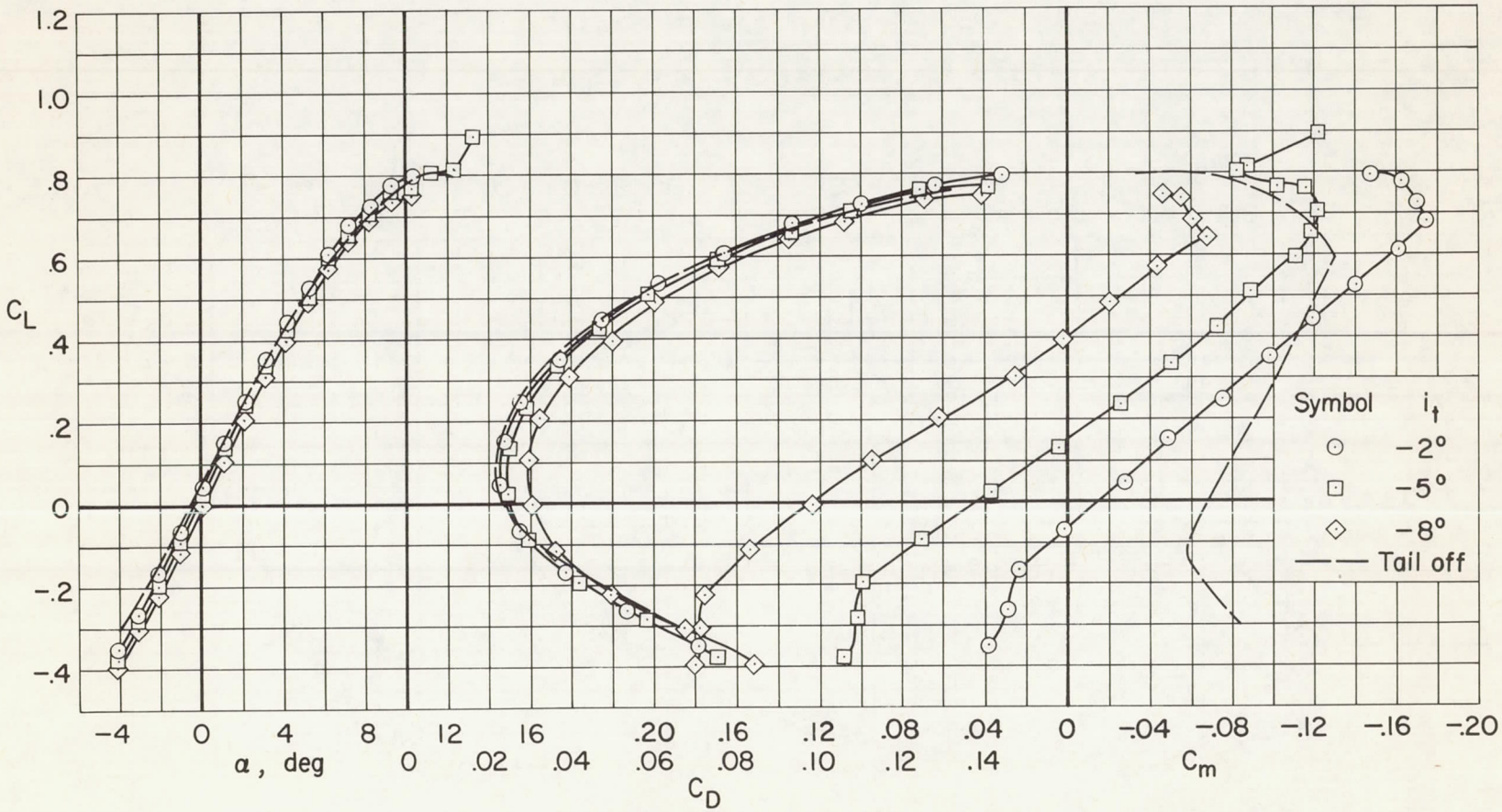

(j) M = 0.92, R = 2,000,000.

Figure 10.- Concluded.

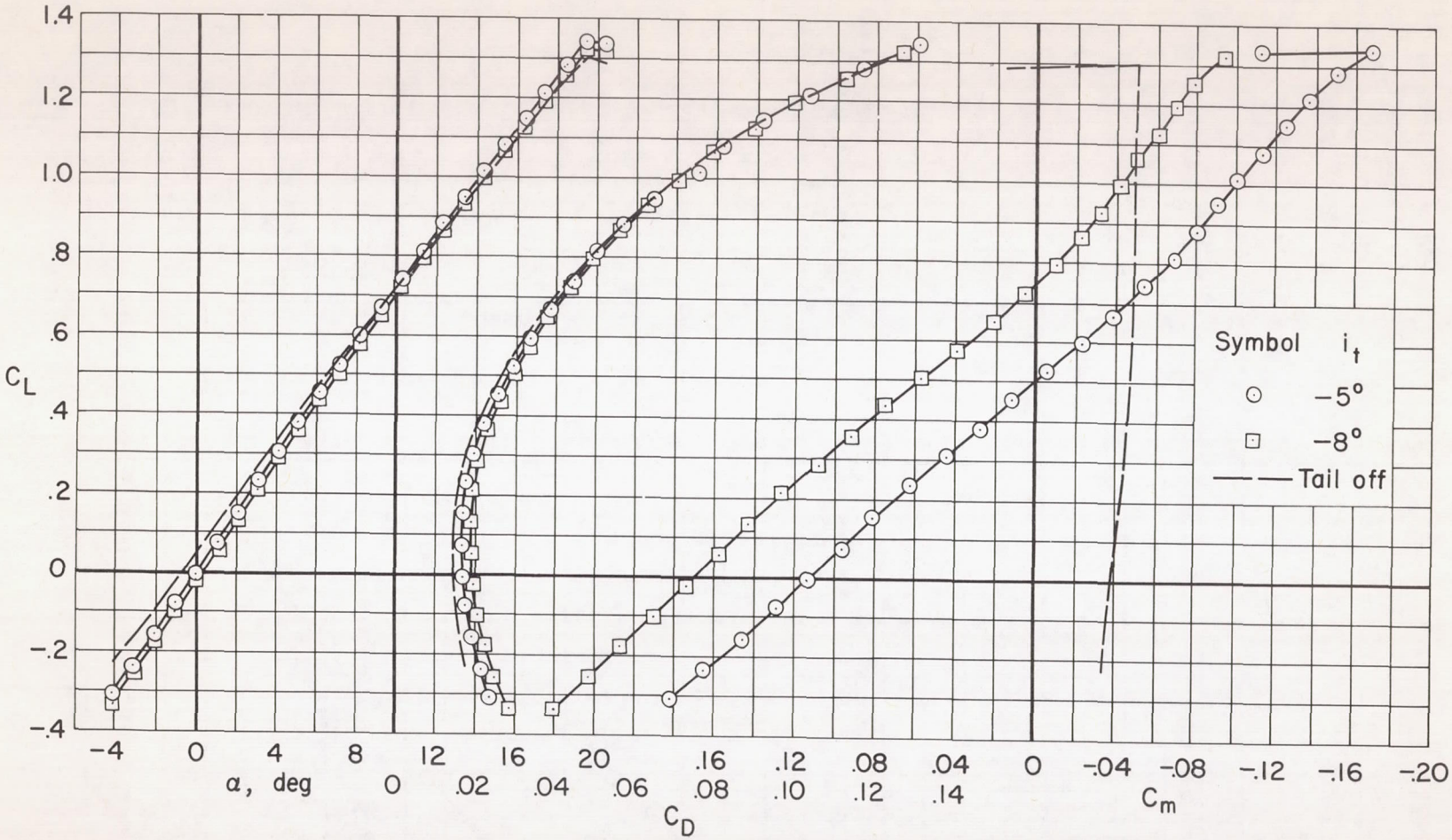

(a) M = 0.25, R = 8,000,000.

Figure 11.- The longitudinal characteristics of the low-wing combination with a horizontal tail at several angles of incidence; tail height = 0.20 b/2.

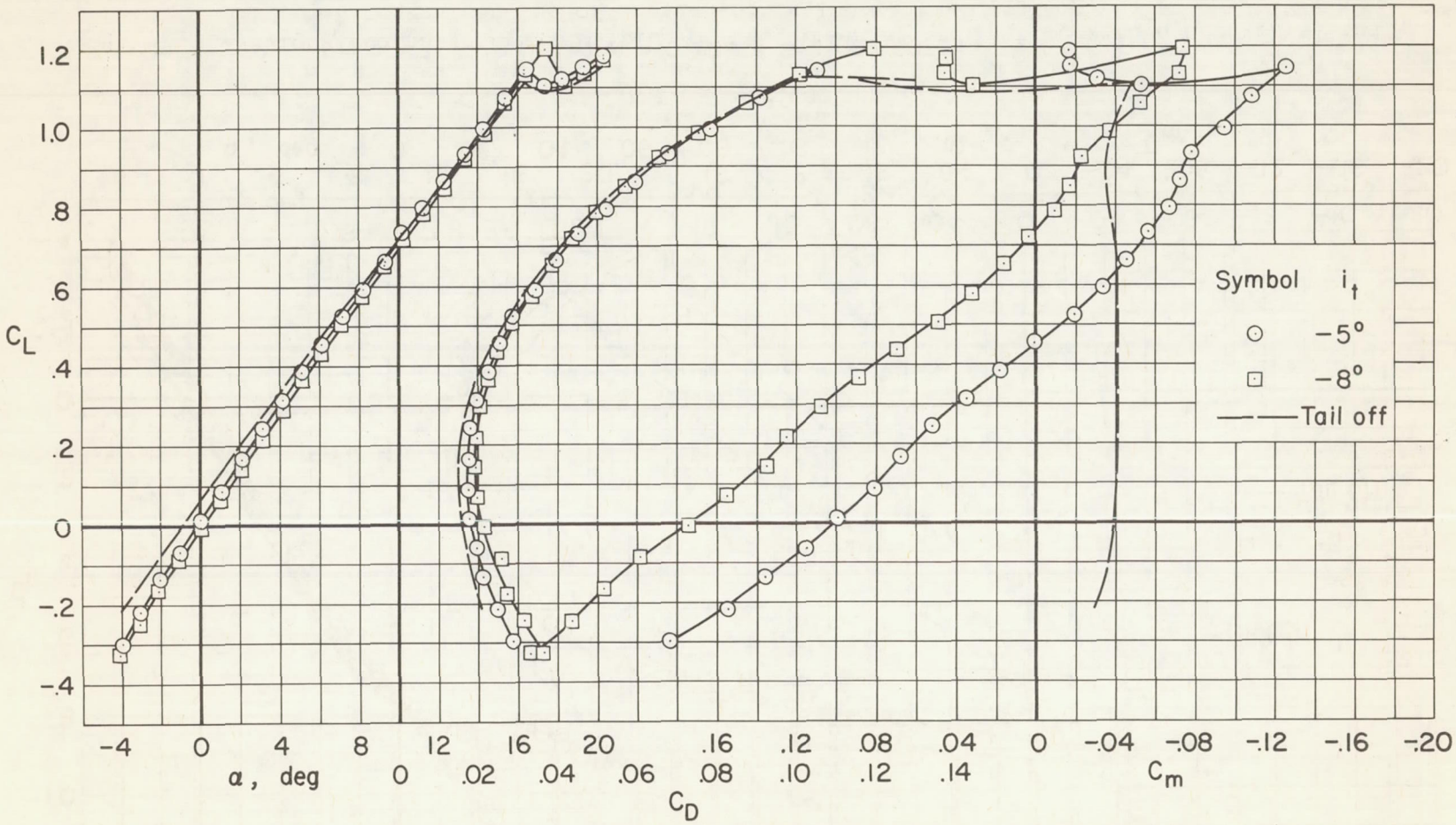

(b) M = 0.25, R = 2,000,000.

Figure 11.- Continued.

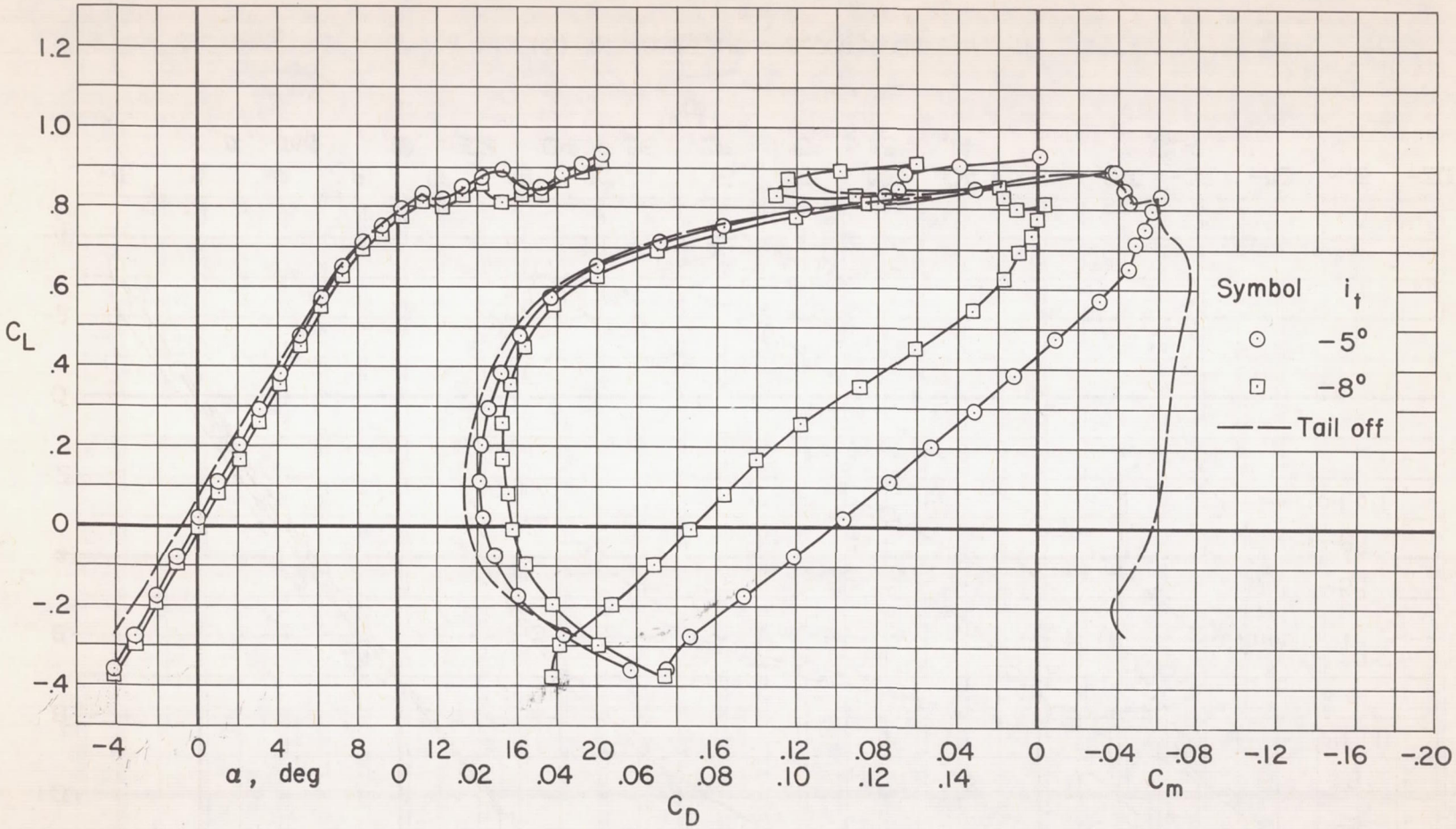

(c) M = 0.80, R = 2,000,000.

Figure 11.- Continued.

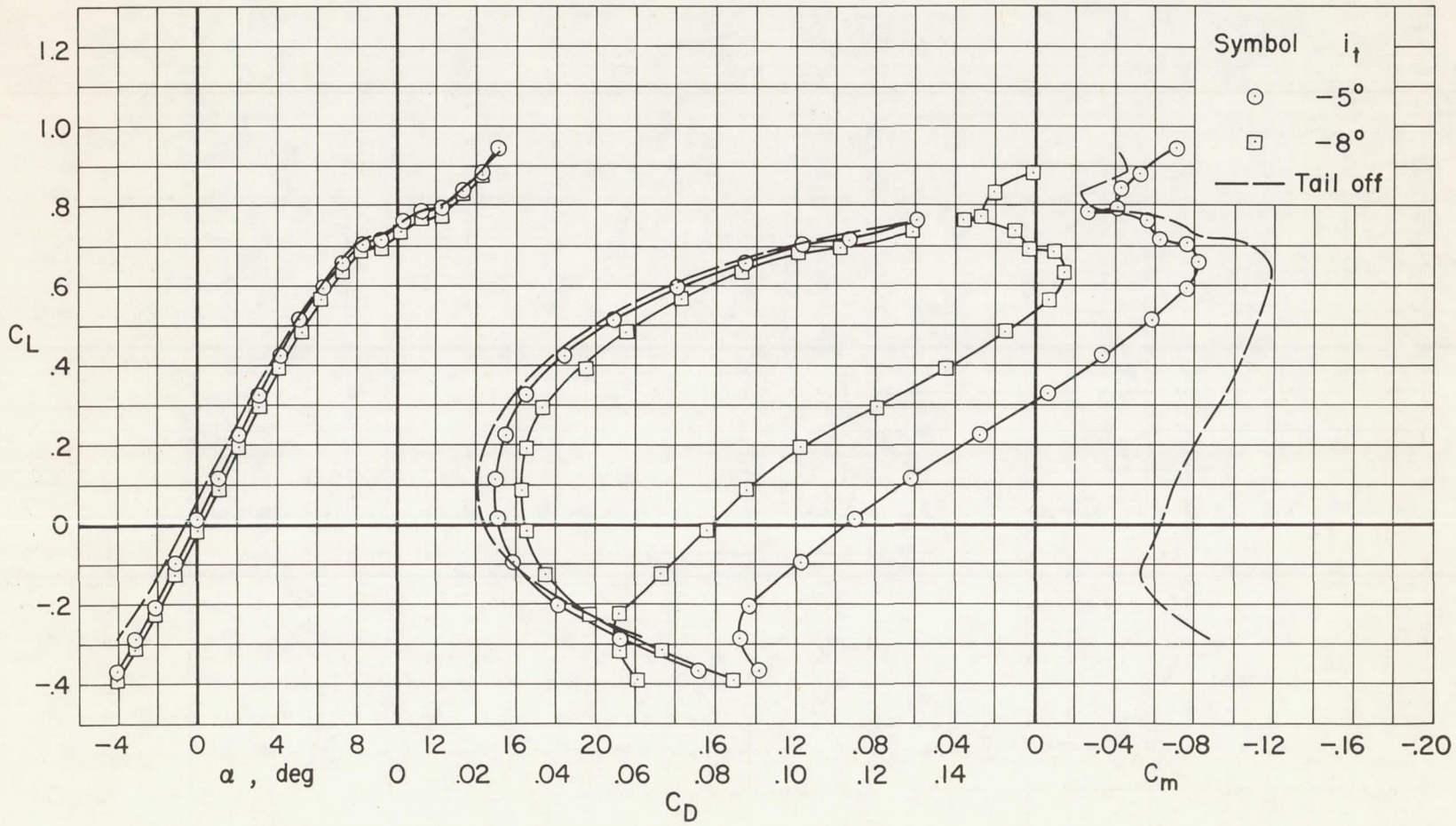

(d) M = 0.90, R = 2,000,000.

Figure 11.- Concluded.

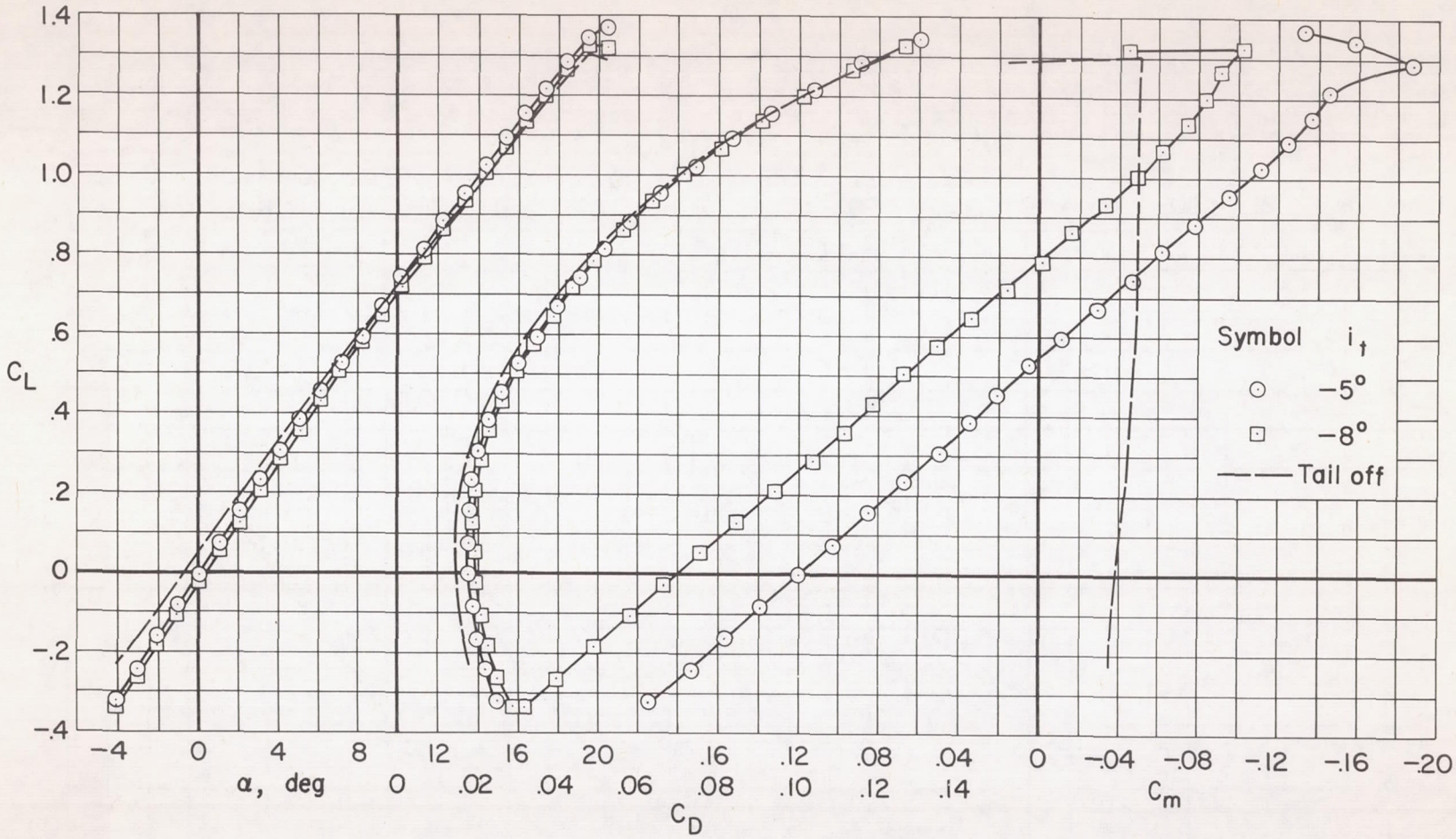

(a) M = 0.25, R = 8,000,000.

Figure 12.- The longitudinal characteristics of the low-wing combination with a horizontal tail at several angles of incidence; tail height = 0.26 b/2.

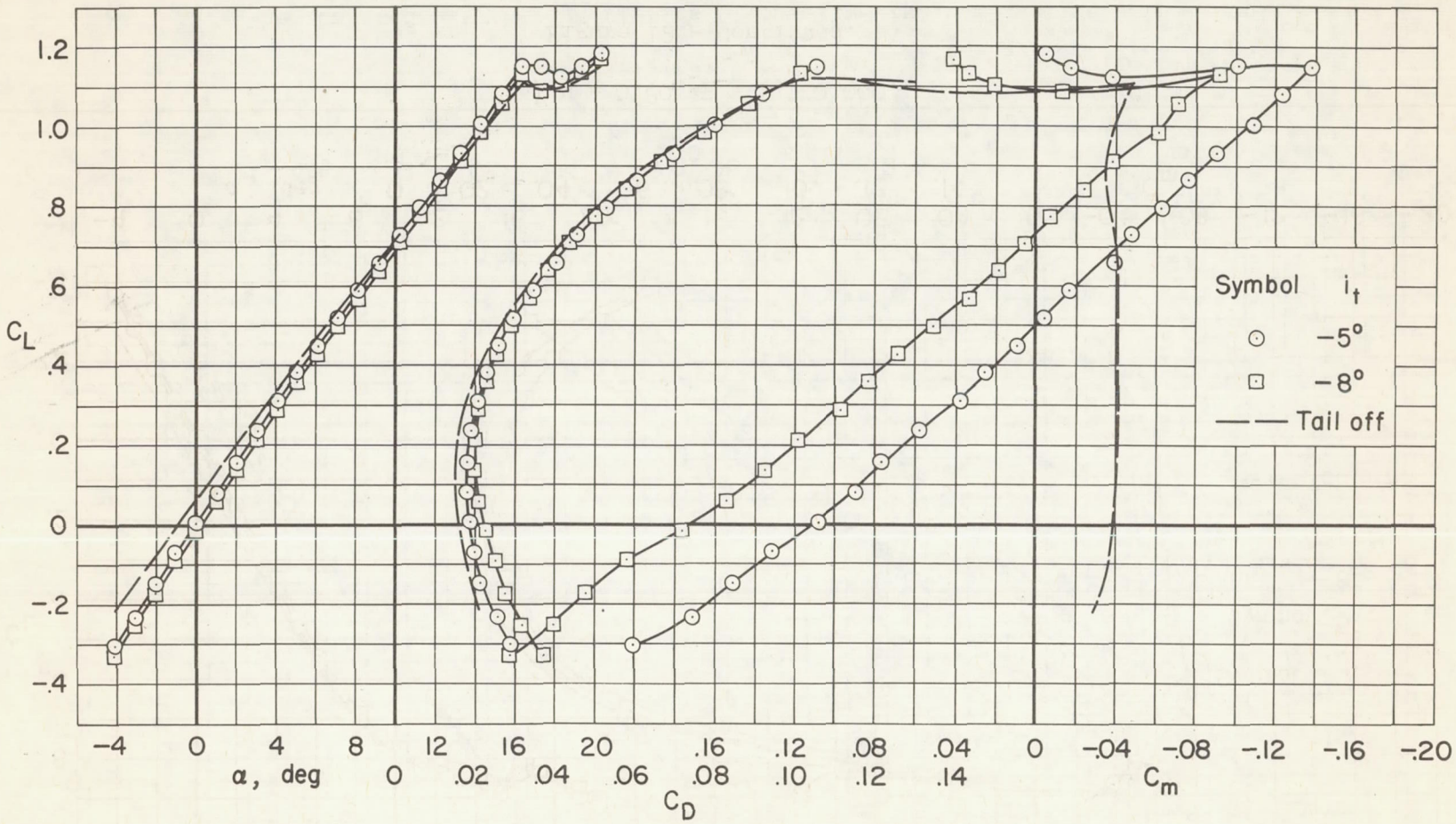

(b) M = 0.25, R = 2,000,000.

Figure 12.- Continued.

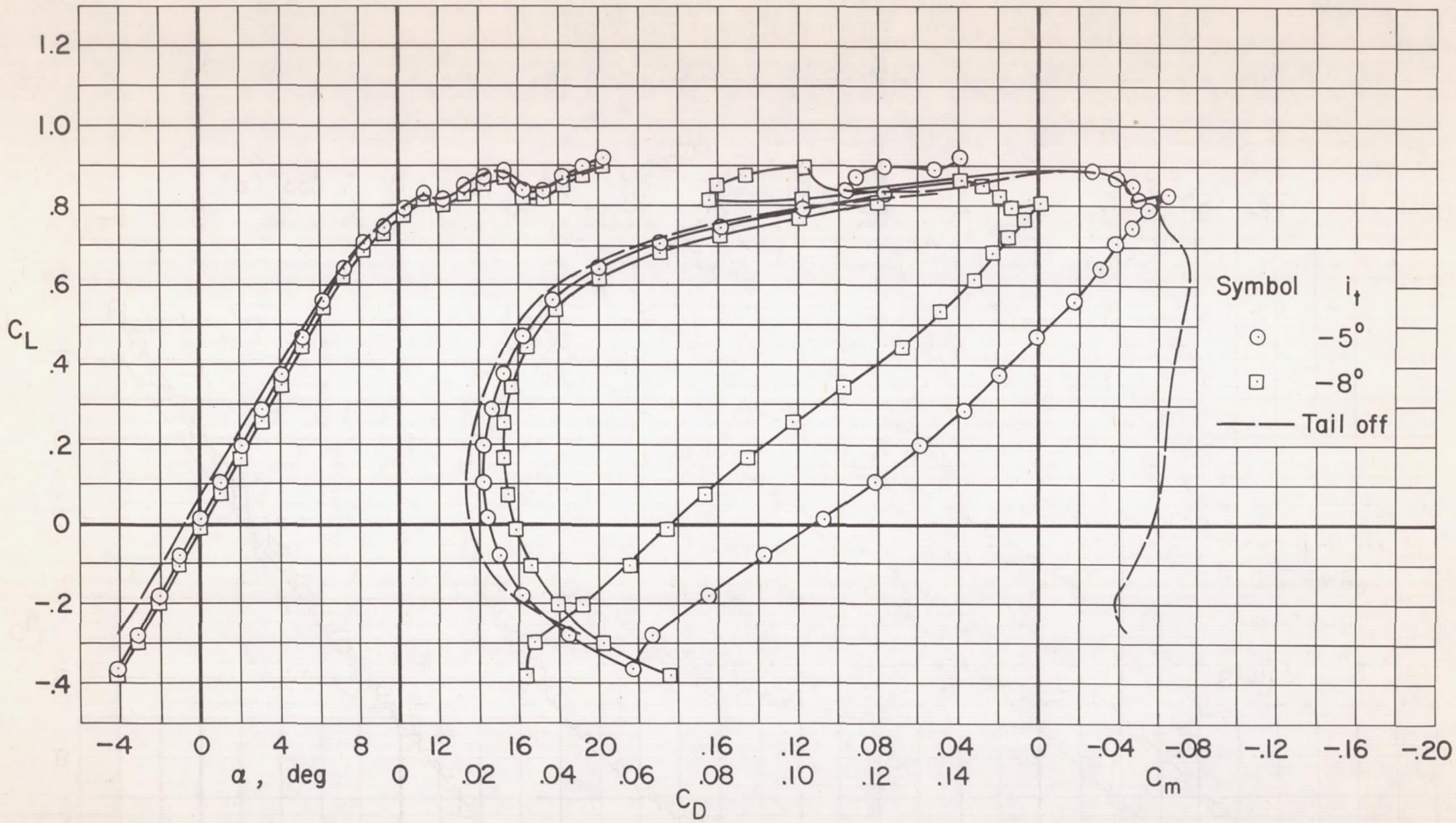

(c) M = 0.80, R = 2,000,000.

Figure 12.- Continued.

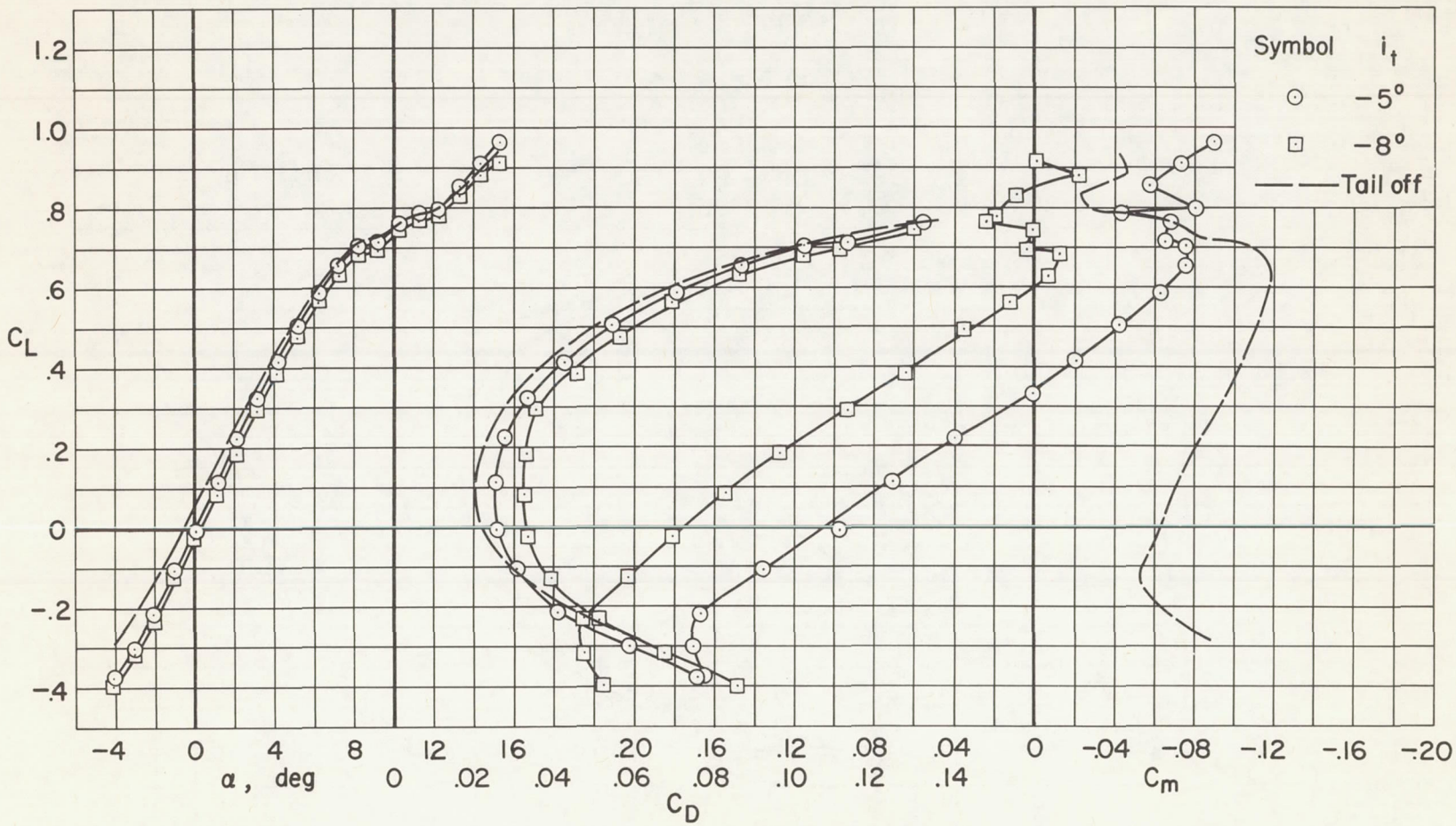

(d) M = 0.90, R = 2,000,000.

Figure 12.- Concluded.

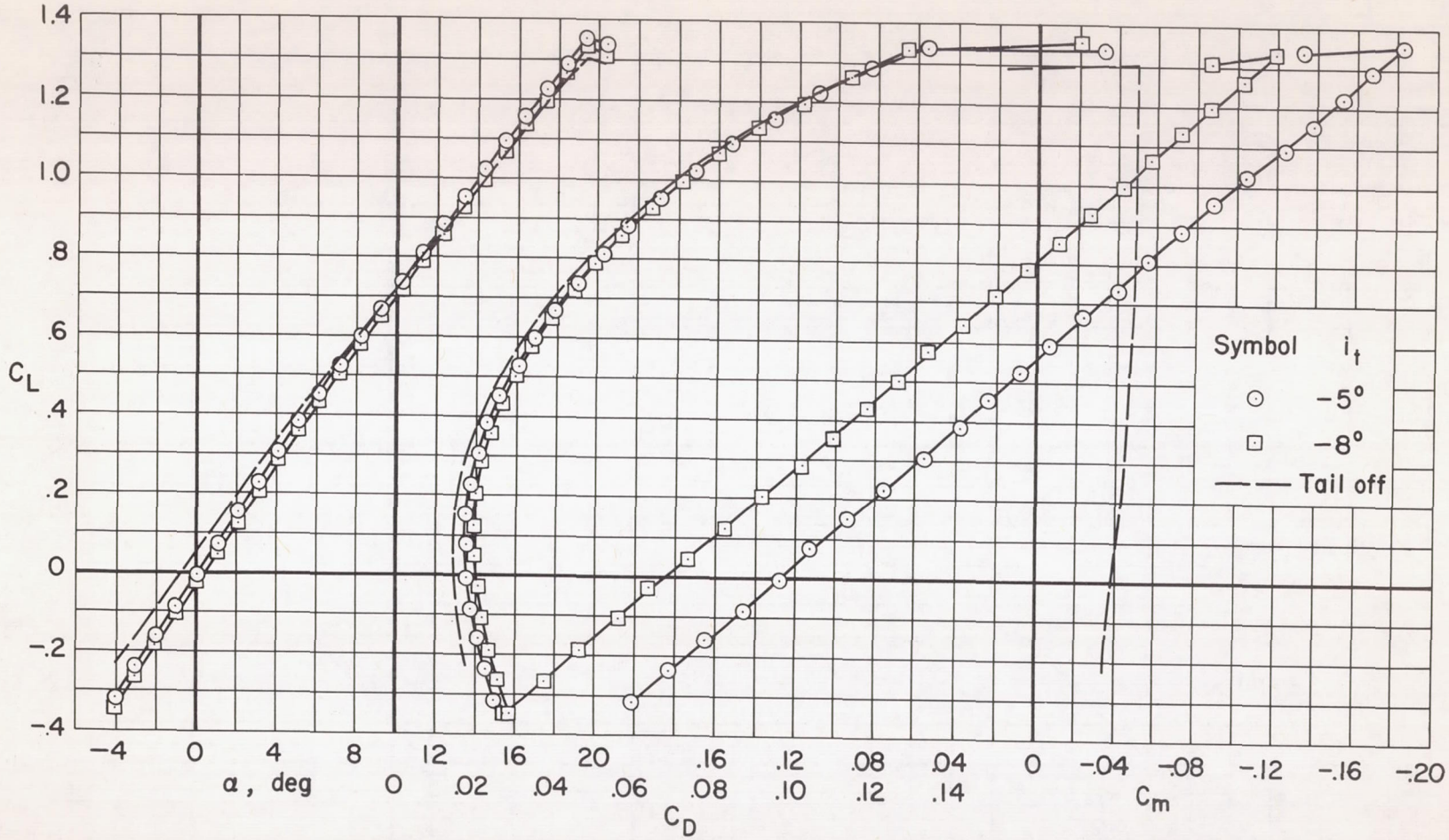

(a) M = 0.25, R = 8,000,000.

Figure 13.- The longitudinal characteristics of the low-wing combination with a horizontal tail at several angles of incidence; tail height = 0.33 b/2.

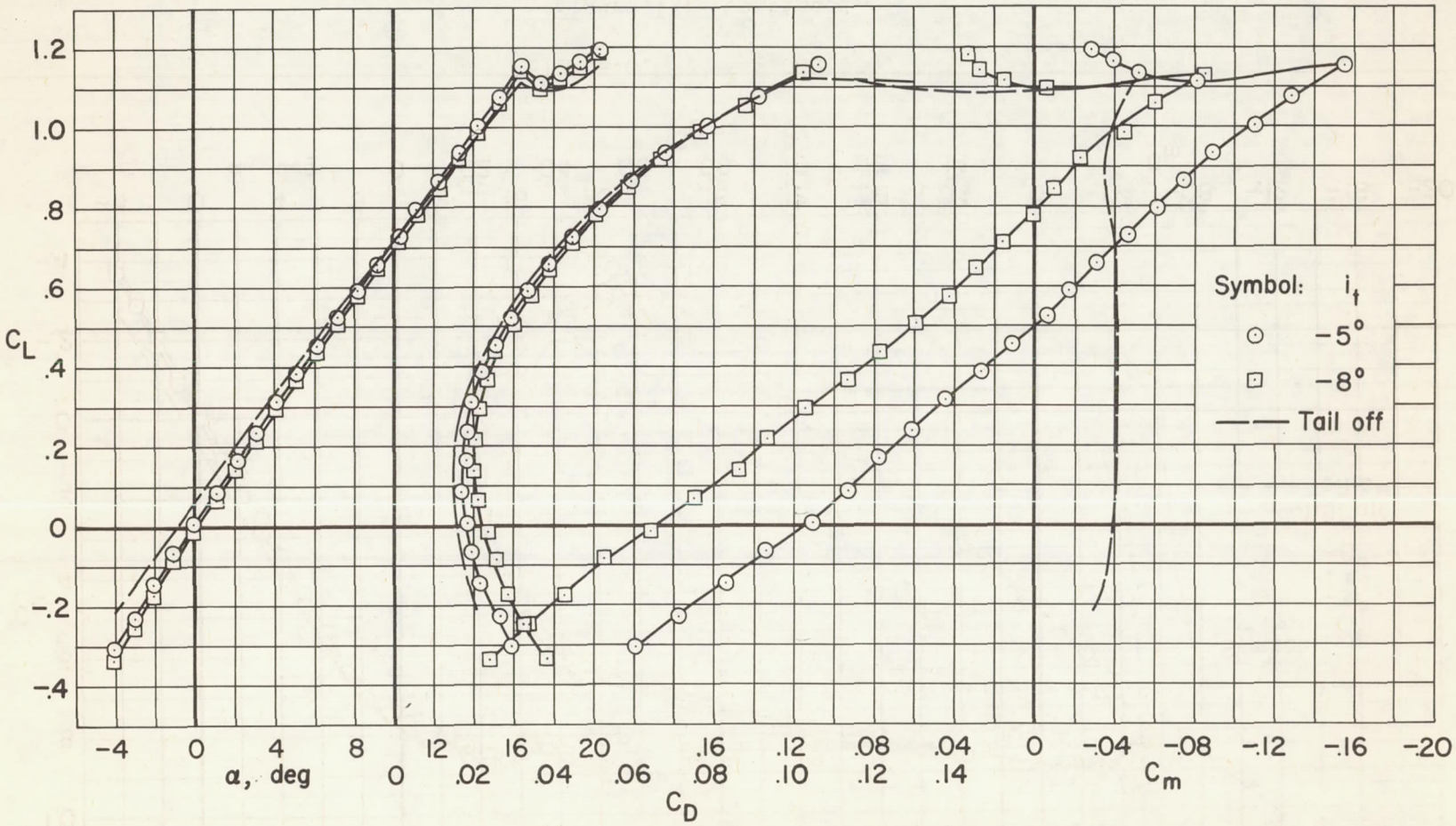

(b) M = 0.25, R = 2,000,000.

Figure 13.- Continued.

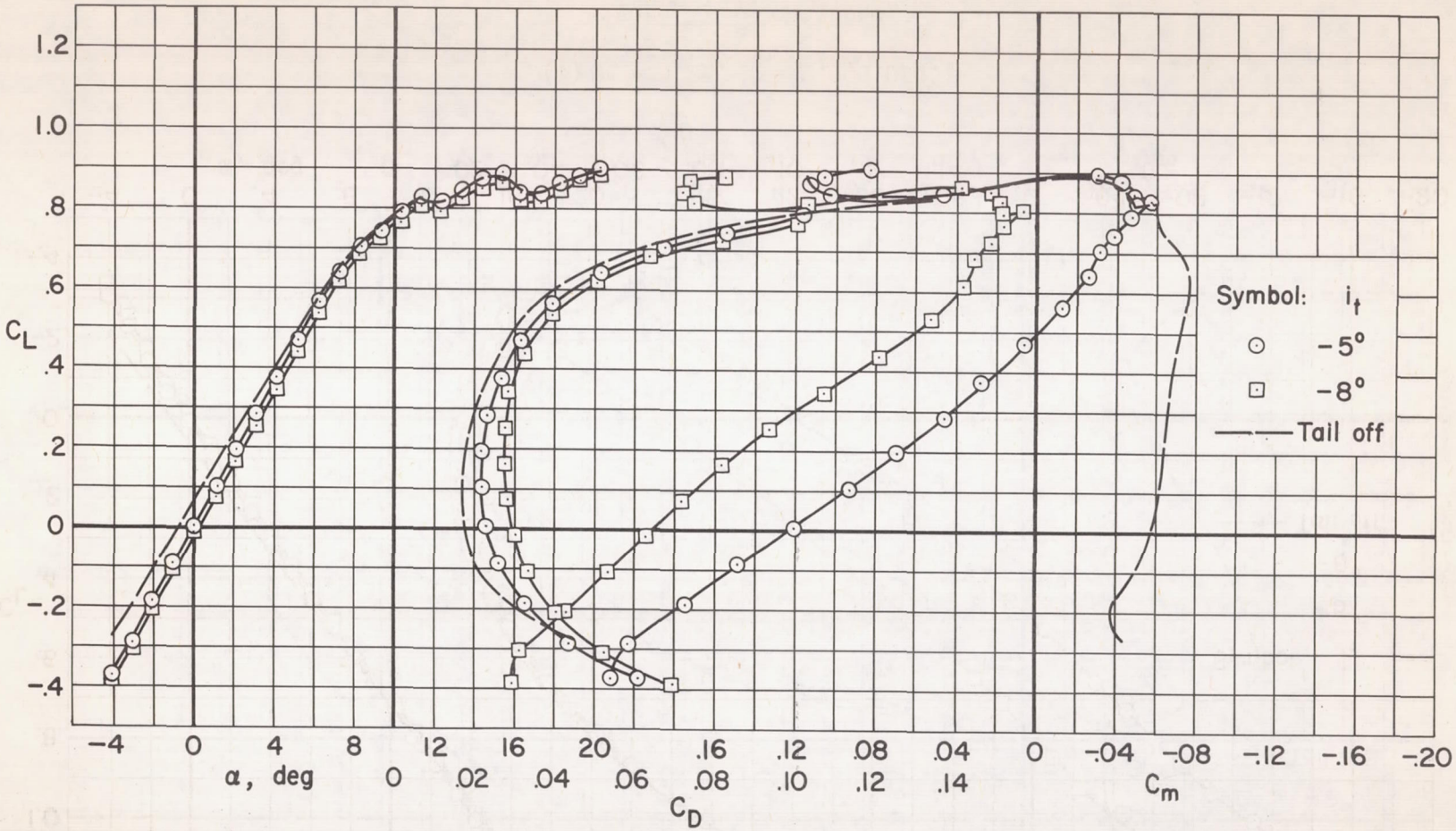

(c) M = 0.80, R= 2,000,000.

Figure 13.- Continued.

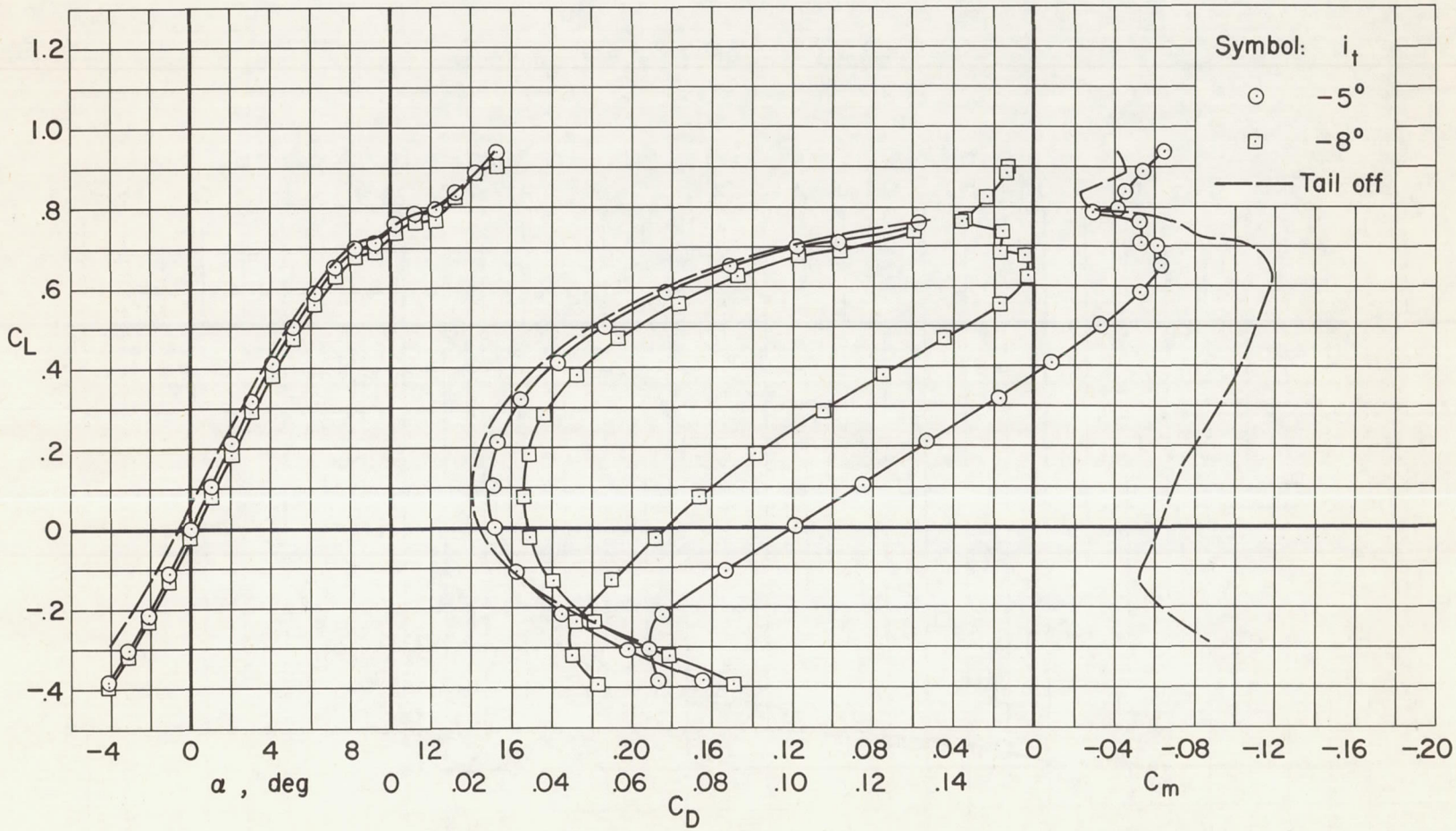

(d) M = 0.90, R = 2,000,000.

Figure 13.- Concluded.

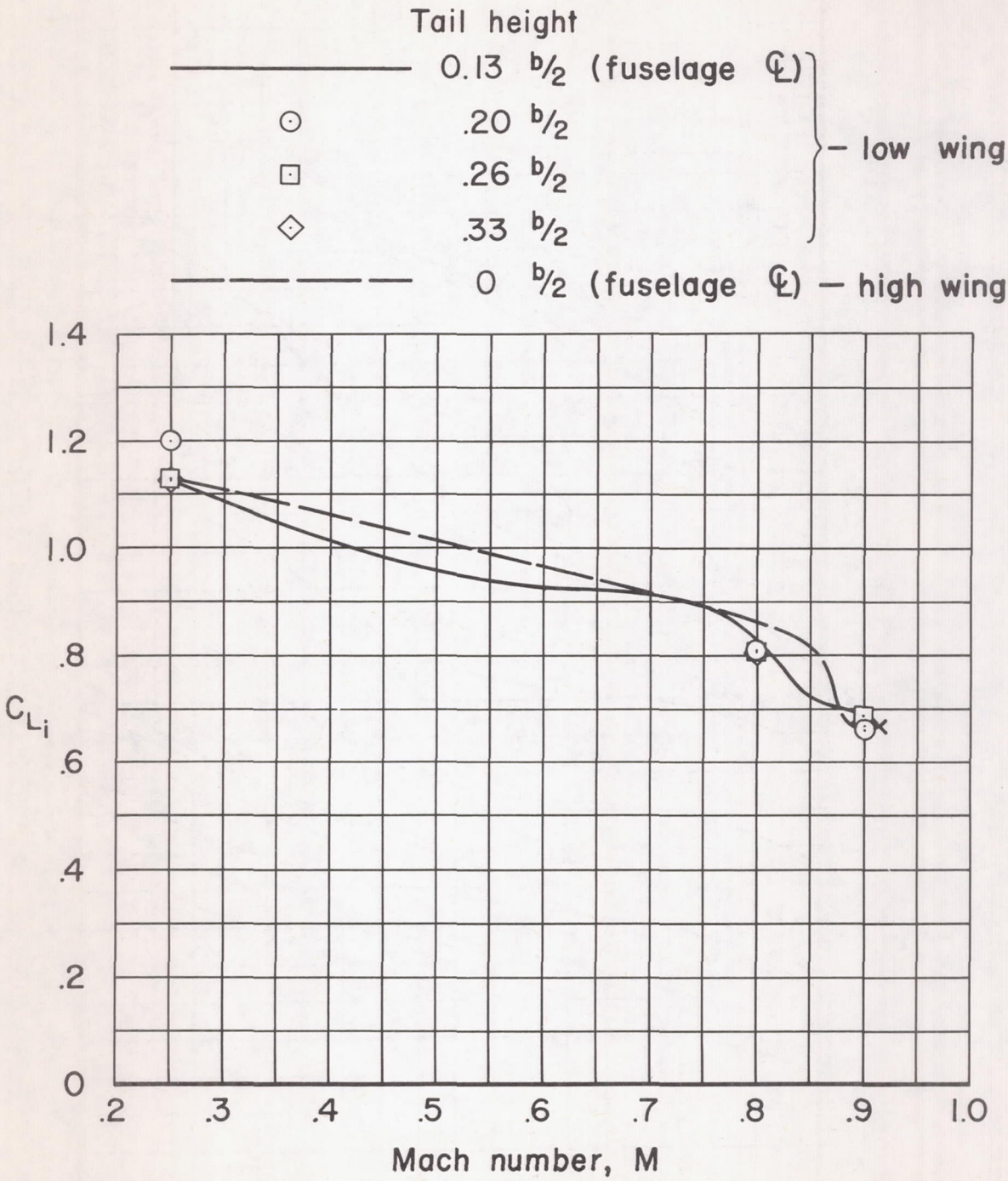

Figure 14.- The variation with Mach number of the inflection lift coefficient for the wing-fuselage-tail combinations; R = 2,000,000; $i_t = -8^{\circ}$.

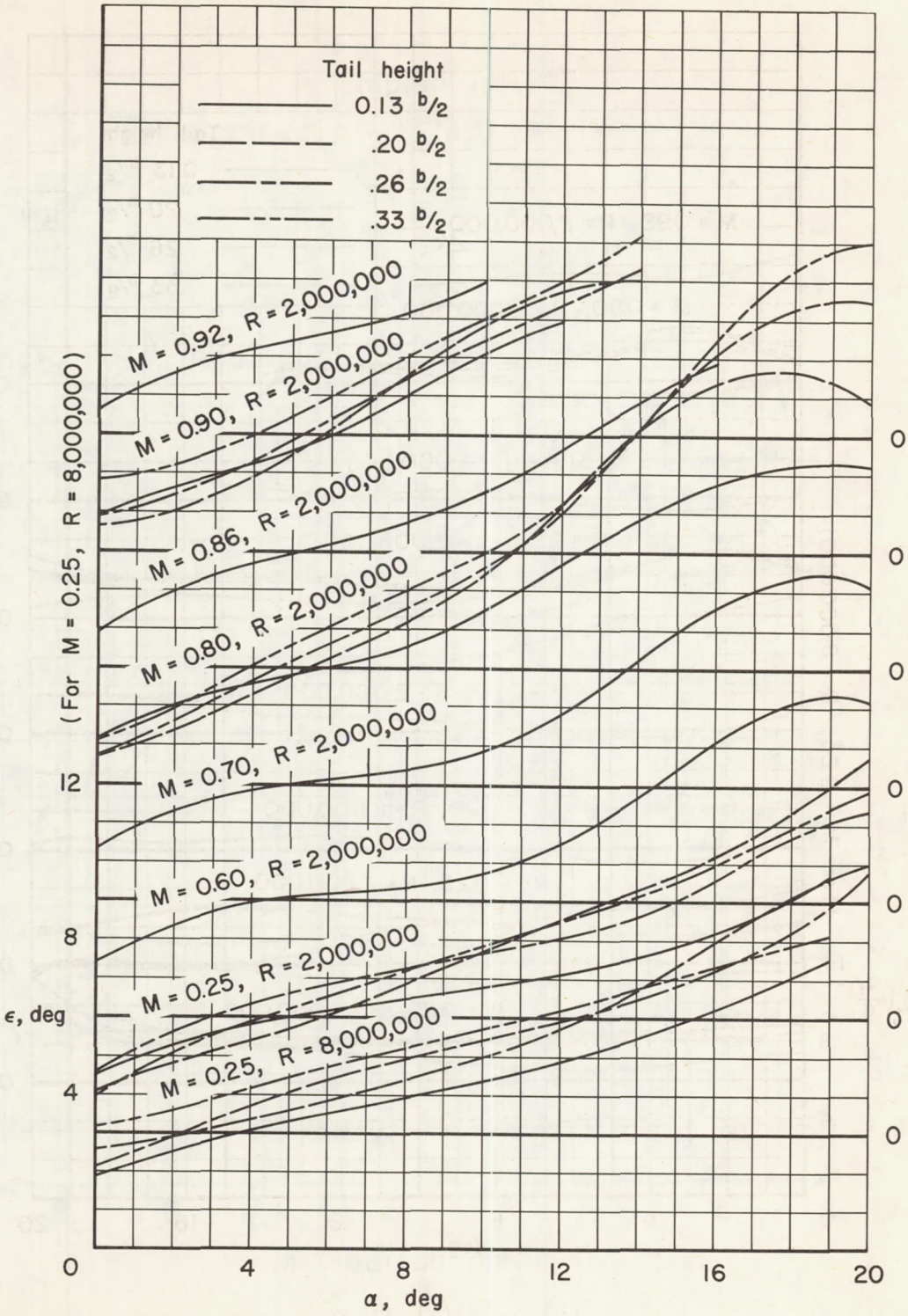

(a) ε vs. α

Figure 15.- The factors affecting the stability contribution of the horizontal tail at several heights for the low-wing combination.

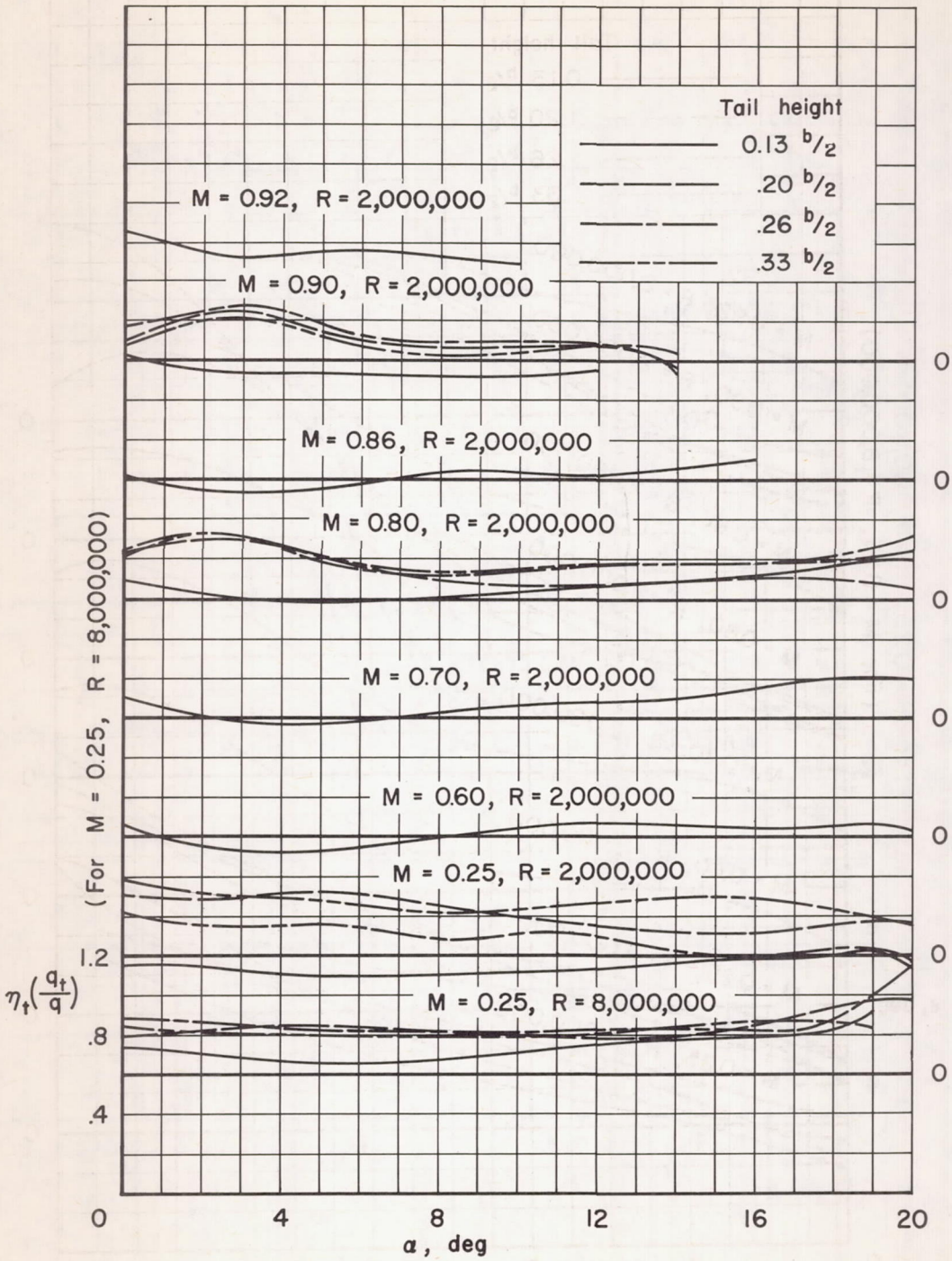

(b) $\eta_t(q_t/q)$ vs. α

Figure 15.- Continued.

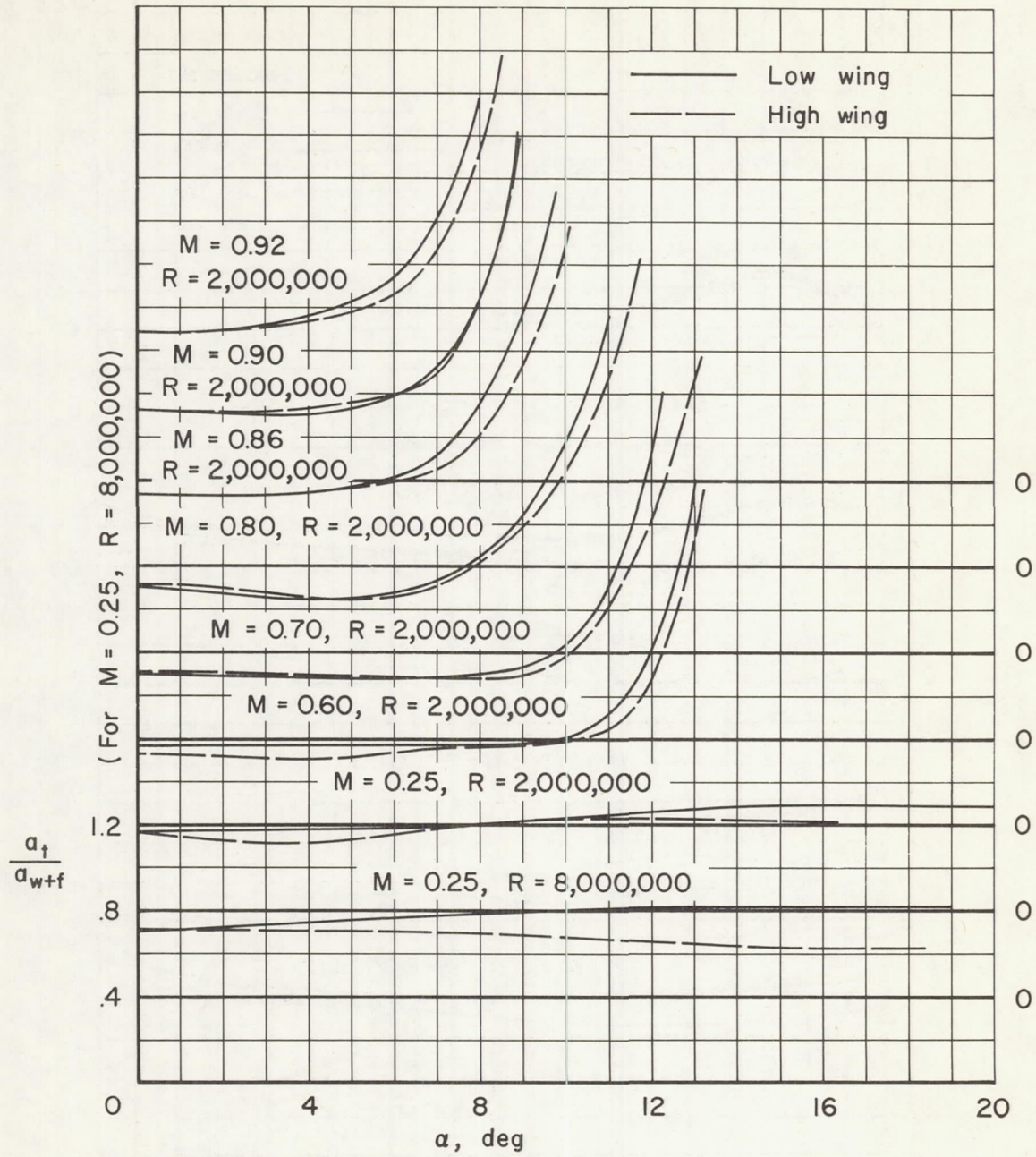

(c) a_t/a_{w+f} vs. α

Figure 15.- Concluded.

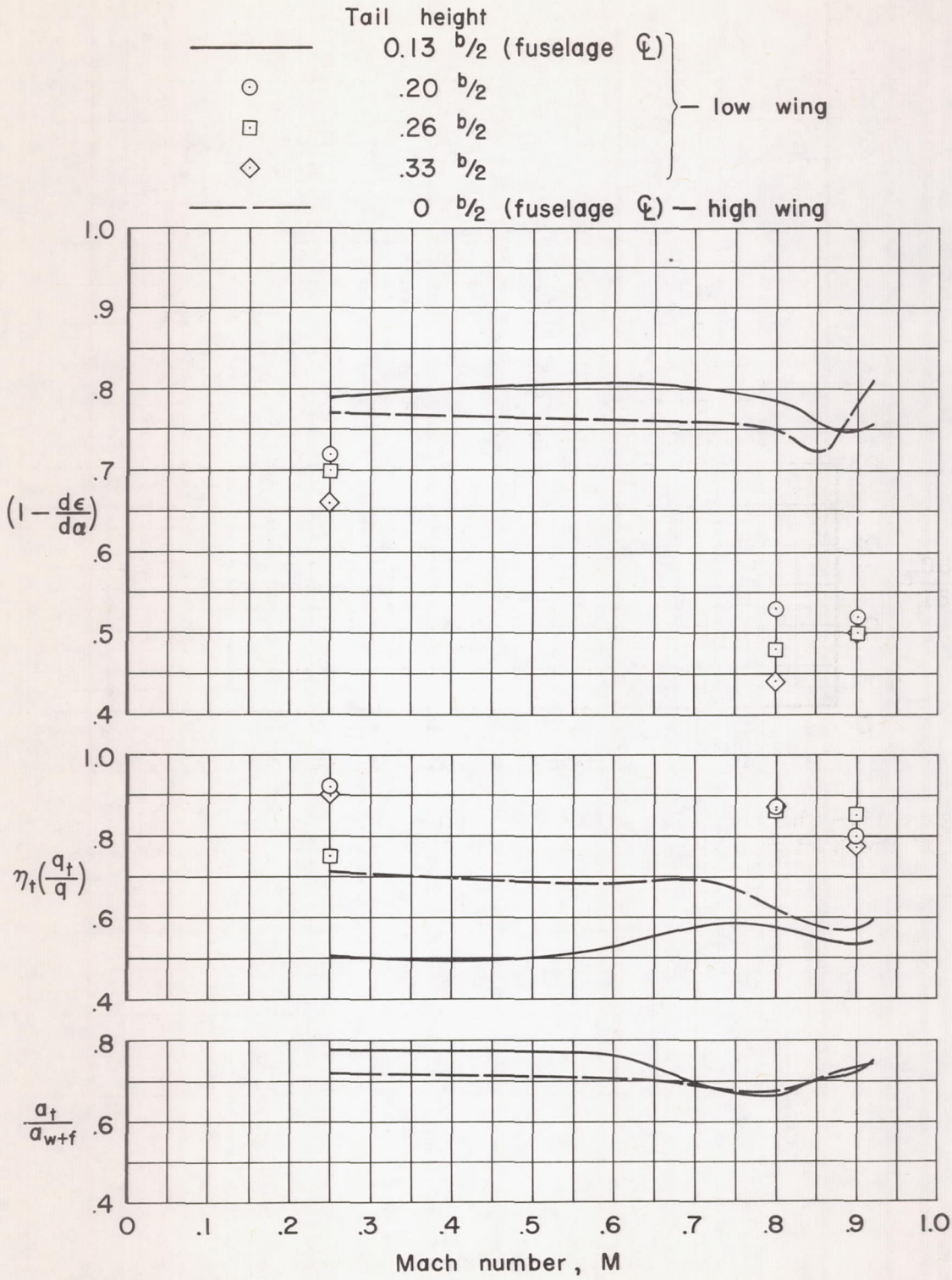

Figure 16- The variation with Mach number of the factors affecting the stability contribution of the horizontal tail at several heights; $\alpha = 4^{\circ}$, R = 2,000,000.

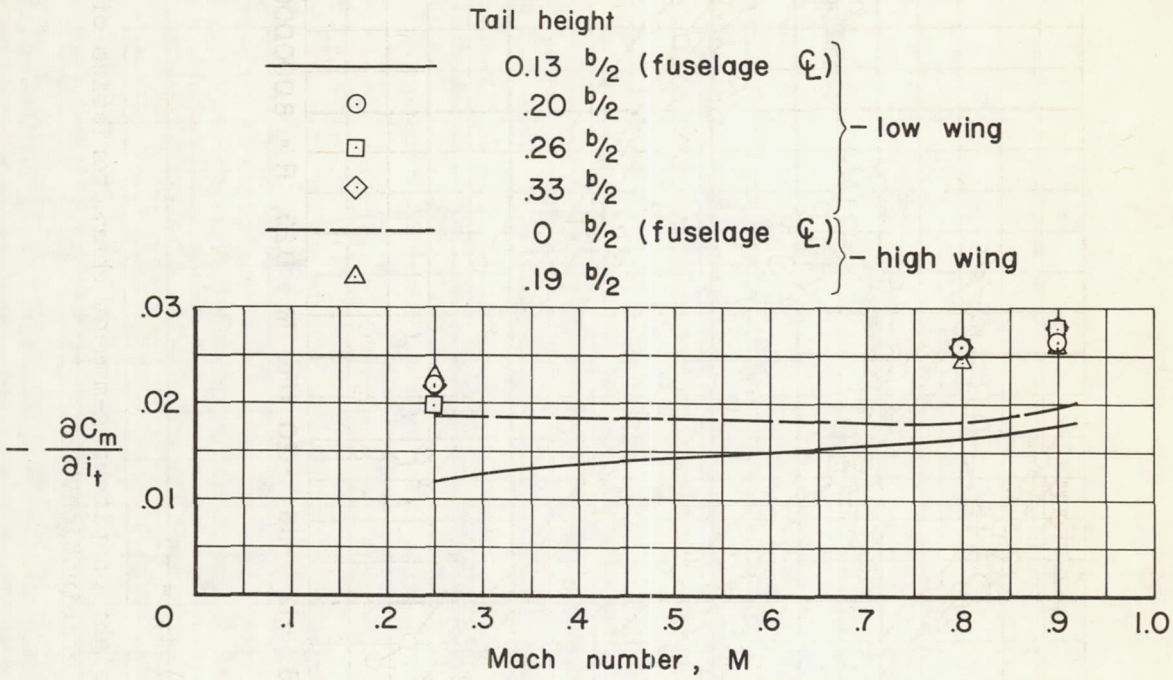

Figure 17.- The variation with Mach number of the control effectiveness of the horizontal tail at several heights; $\alpha = 4^{\circ}$, R = 2,000,000.

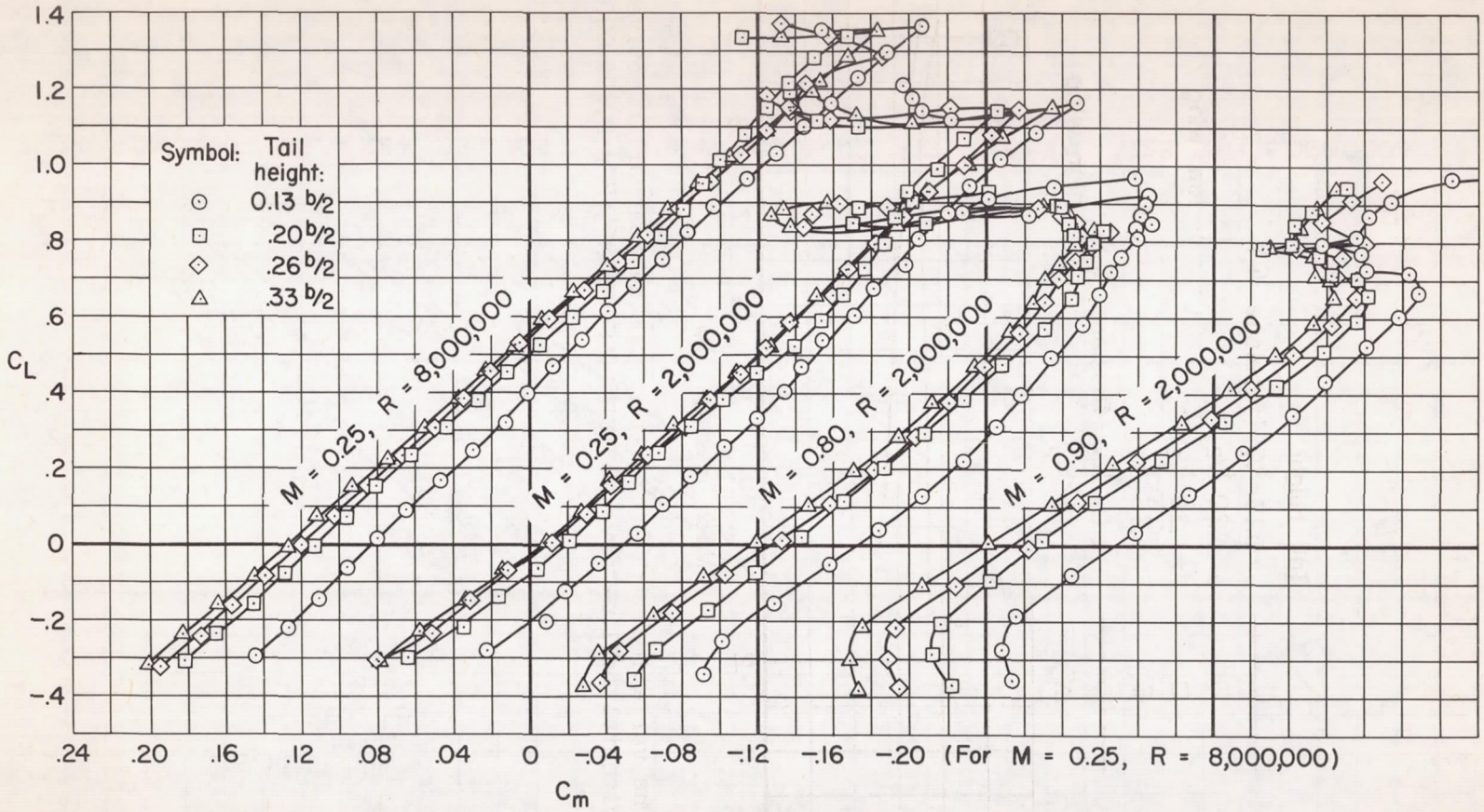

(a) $i_t = -5^\circ$

Figure 18.- The effect of horizontal tail height on pitching-moment characteristics of the low-wing combination.

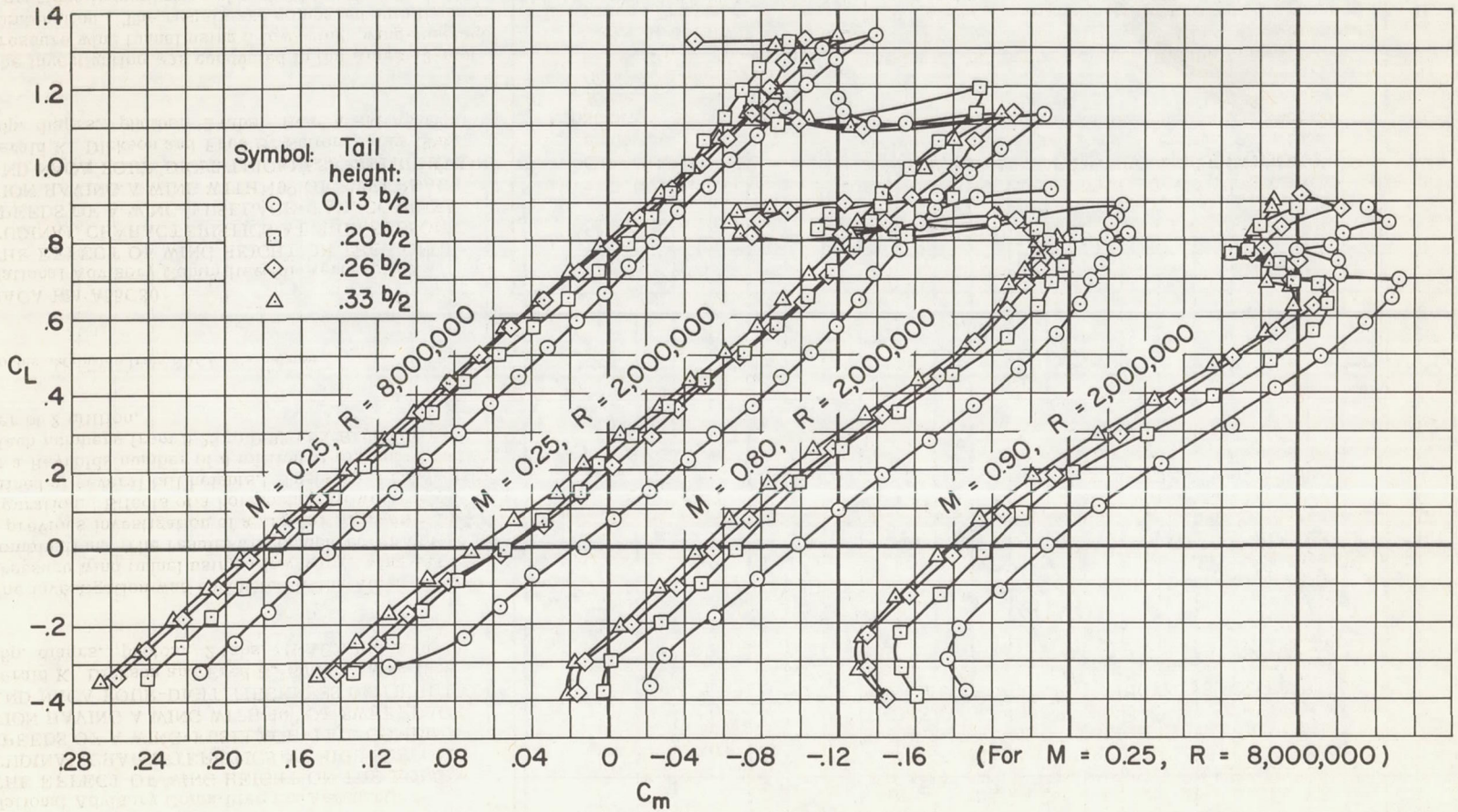

(b) $i_t = -8^{\circ}$.

Figure 18.- Concluded.